Electrochemically Enhanced Reduction of Iron Oxide from Slag

by

David Edward Woolley

S.B. Materials Science and Engineering, MIT, 1993

S.B. Mathematics, MIT, 1993

Submitted to the Department of Materials Science and Engineering
in Partial Fulfillment of the Requirements for the Degree of

Doctor of Philosophy

at the

MASSACHUSETTS INSTITUTE OF TECHNOLOGY

February 1998
[June 1998]

Author _____
Department of Materials Science and Engineering
January 9, 1998

Certified by _____
Uday B. Pal
Associate Professor of Chemical Processing of Materials
Thesis Supervisor

Accepted by _____
Linn W. Hobbs
John F. Elliott Professor of Materials
Chairman, Departmental Committee on Graduate Students

Electrochemically Enhanced Reduction of Iron Oxide from Slag

by

David Edward Woolley

Submitted to the Department of Materials Science and Engineering on January 9, 1998, in partial fulfillment of the requirements for the degree of Doctor of Philosophy in Materials Engineering

---

Abstract

An experimental study was performed to measure the rate of reduction of iron oxide from calcia-silica-alumina slag by carbon in iron, and to determine whether the reaction rate can be increased by electrochemical means. It is shown that the reaction rate depends on both the ferric-ferrous cation ratio, and on the total amount of iron in the slag. It was observed that ferric cations are reduced at a faster rate than ferrous cations. This suggests that the overall reaction rate is limited by the rate of the ferric-to-ferrous reduction reaction when the slag contains significant quantities of ferric oxide. Results show that the rate constant decreases at low concentrations of ferrous oxide in the slag. It is concluded that mass transfer in the slag phase controls the overall reaction rate when the slag contains mainly ferrous oxide.

Experiments were conducted in an attempt to increase the reaction rate by electrochemical means. The reaction rate was increased by penetrating the slag layer with a metallic rod or plate; this provided an electronic pathway from the metal bath into the bulk slag phase. A small short-circuit current was measured. In order to increase the current, a voltage was applied between the metal bath and an electrode that made electrical contact with the top of the slag layer. The reaction rate increased by 60-100%, and the increase was proportional to the current passed. A current efficiency of nearly 100% was observed for current densities on the order of 500 mA cm^{-2}.

The results of this study have been modeled with a new expression for the reaction rate:

$$r_O = k_1\left[wt.\%Fe^{3+}\right]_{slag} + k_2\left[wt.\%Fe^{2+}\right]_{slag}$$

The rate constant k_1 is the chemical rate constant for the ferric-to-ferrous reduction reaction, and k_2 is the mass transfer coefficient for ferrous cations in the slag; numerical values for the constants k_1 and k_2 are offered for certain experimental conditions.

Thesis Supervisor: Uday B. Pal
Title: Associate Professor of Chemical Processing of Materials

Table of Contents

List of Figures

List of Tables

Acknowledgments

First, I would like to thank my wife and my parents. I value their love and support more than anything else.

I wish to acknowledge my Thesis Advisor, Prof. Pal, for his advice and encouragement. My time spent in his High Temperature Materials Process Technology Group has been of great benefit to me.

Dr. Harold Larson has helped me in many ways with this project. I wish to thank him for all the kindness and patience he has shown me.

Professor Julian Szekely was my Thesis Advisor from the time I began graduate school until his passing in December, 1995. I have many fond memories of him, and my time in his Materials Process Modeling Group.

I would like to acknowledge the support I have received from the other students and researchers in Professor Pal's laboratory: Prashant Soral, Ashish Agarwal, Stephen Britten, Dr. Sridhar Seetharaman, Dr. Victor Stancovski, and Dr. Kuo-Chih Chou. Prashant helped me in many ways to finish my thesis; I feel lucky to have met such a friend.

I wish to thank the members of my thesis committee: Prof. Sadoway, Prof. Rose, and Prof. Pal for their advice and suggestions. I appreciate very much the time they have devoted to my education.

I would like to thank Prof. Alex McLean from the University of Toronto for helping me with my thesis and with various papers and presentations. I feel privileged to have been able to learn from him during his sabbatical stay at MIT in the fall of 1997.

Finally, I acknowledge financial support from the National Science Foundation, under award number DMI-9528635.

Chapter 1. Introduction

1.1 Motivation for the present study

In modern steelmaking, the final iron oxide content of slags is in the range 5-35 wt% 'FeO' in the basic oxygen furnace (BOF), and 10-40 wt% 'FeO' in the electric arc furnace (EAF), depending on the final carbon content of the steel. Most steelmaking slag is not recycled; impurities in the slag limit the amount that can be recycled into the blast furnace or steelmaking furnace. It would be desirable if the 'FeO' level in the slag could be reduced before the slag is discarded (i.e. lost from the iron- and steelmaking process), since this would improve iron yield.

The 'FeO' content of steelmaking slags could be decreased by the reaction in Equation (1), in which iron oxide is reduced from slag by reacting with carbon dissolved in liquid iron.

$$[FeO]_{slag} + [C]_{metal} \rightarrow [Fe]_{metal} + (CO) \qquad (1)$$

In order to make this practical, conditions must be maintained so that the rate of this slag-metal reaction is high. The original motivation for this study was to see whether some electrochemical means involving an electric arc or a plasma might be developed that would increase the reaction rate (see Background below).

This slag-metal reaction is important in both iron- and steelmaking and has therefore been the subject of study previously. Early studies of the reaction rate were motivated by the desire to understand the reaction as it occurs in the hearth of the blast furnace, and in basic open hearth steelmaking. Most studies in the past twenty years have aimed at learning about the reaction as it occurs in steelmaking in the BOF and EAF, and in direct smelting processes for ironmaking.

In pneumatic steelmaking processes, oxygen gas is blown into hot metal in order to oxidize carbon, silicon, phosphorus, and other impurities. Slag droplets are formed at the gas entrance into the metal bath. Iron oxide in the slag droplets is reduced by carbon dissolved in the metal bath (Equation (1)) as the droplets rise upward through the metal bath to the slag layer. The fluid flow pattern in the reactor influences the iron oxide content of the slag[1,2], as does the total amount of oxygen blown into the metal bath[3].

In direct smelting processes for ironmaking, molten iron is produced using ore, coal, and flux[4]. As in the blast furnace, some reduction occurs by reaction between solid ore and gas containing carbon monoxide and hydrogen. At the bottom of the furnace, however, where hot metal and slag accumulate, reduction occurs by the reaction in Equation (1).

Previously published studies have shown that a high reaction rate is obtained under the following conditions:

- high iron oxide concentration in the slag phase[5]

- high temperature[6]
- vigorous stirring of the slag and metal phases[6,17]
- high carbon concentration (in the metal phase)[7]

These studies provide a basic understanding of the reduction of ferrous oxide (FeO) from slag. They do have some short-comings, however.

Most studies to date have neglected the effect of ferric oxide (Fe_2O_3) on the reaction rate; in fact, they have purposely used slags that only contain FeO. A second short-coming of previous studies is that they have treated this slag-metal reaction as a chemical reaction, as if it were occurring between the compound FeO and carbon. It is known, however, that iron oxide is dissociated in slags, so that the reduction of iron oxide probably occurs as anodic and cathodic reactions. In the anodic reaction, oxygen from the slag reacts with carbon dissolved in the metal bath.

$$\left[O^{2-}\right]_{slag} + [C]_{metal} \rightarrow (CO) + 2e^{-} \tag{2}$$

If both ferric and ferrous cations are present in the slag, then two cathodic reactions are possible. One is the reduction of ferric cations to ferrous cations

$$\left[Fe^{3+}\right]_{slag} + e^{-} \rightarrow \left[Fe^{2+}\right]_{slag}, \tag{3}$$

and the other is the reduction of ferrous cations to iron metal

$$\left[Fe^{2+}\right]_{slag} + 2e^{-} \rightarrow [Fe]_{metal}. \tag{4}$$

A third deficiency in previous studies is that they have generally focused on one of the following two extremes:

- low carbon concentration, and high iron oxide concentration;
- low iron oxide concentration, and high carbon concentration.

The first type of study, on "decarburization," often involves dropping solid iron pieces or molten iron droplets into a slag layer. The second type of study, on "iron oxide reduction," usually involves dropping crushed or molten slag onto a molten iron layer.

In this study, two of these three deficiencies have been treated. First, the effect of ferric cations on the rate has been explicitly studied. Second, the reduction of iron oxide from slag by carbon in iron (Equation (1)) has been studied from an "electrochemical" point-of-view, and experiments have been conducted to show that the overall reduction reaction is indeed occurring as separate oxidation and reduction reactions (Equations (2), (3), and (4)). In order to focus on rate-limitations in the slag phase, high carbon concentration has been employed; iron oxide reduction experiments have been conducted.

1.2 Background to present study

A study by Krishna Murthy, Hasham, and Pal[8] showed that the rate of decarburization of iron droplets slowed to nearly zero when the carbon level reached 2-3 wt%, even though the slag still contained a high level of FeO. When the crucible (containing the molten slag) was lined with molybdenum foil, the carbon level reached almost 0 wt%. The investigators suggested that "an electrochemical transport barrier in the slag phase" was preventing the final carbon level from dropping below 2-3 wt% when no foil was present.

They proposed that electrons were built up in the metal droplet, because iron cation diffusion was slower than oxygen anion diffusion to the surface of the metal droplet. This electron build-up would eventually present a barrier to oxygen anion diffusion to the droplet, and the decarburization rate would drop to nearly zero. They suggested that the foil "drained" electrons away from the metal droplet, so that oxygen anions could once again diffuse to the surface of the droplet, and the reaction could proceed to 0 wt% C. Szekely and Pal[9] later proposed that an electronic short-circuit through the slag layer using an electric arc or plasma might increase the reaction rate in a similar manner.

This study was initially undertaken to study the effect of electrically "short-circuiting" the slag layer, as was done with molybdenum foil in the study by Krishna Murthy et al. Two goals were defined. The first was to confirm that the rate is increased by electrically short-circuiting the slag with a metallic conductor. The second was to show that the rate could be increased by short-circuiting the slag layer with an electric arc or plasma column. The experimental plan, in both cases, was to measure the reaction rate with and without electrically short-circuiting the slag to show that the reaction rate is higher with short-circuiting.

Before the experimental program began, the literature was reviewed to see if any other investigators had seen the rate of decarburization stop at high values of carbon in the metal, even though the slag contained significant quantities of FeO. This exercise

revealed that Gare and Hazeldean[10] had observed that the decarburization rate of iron droplets slowed to nearly zero when the carbon level reached 3 wt%. They noticed that this occurred when the slag initially contained a high ratio of ferrous-to-total iron, in the range 0.44-0.5. When the slag initially contained a lower ratio of ferrous-to-total iron, in the range 0.15-0.28, the carbon level decreased to nearly 0 wt% in their experiments. This study suggested to the author that a study focusing of the role of ferric cations was necessary.

Further review of the literature showed that Mulholland, Hazeldean, and Davies[7] had made qualitative observations of the rate of decarburization of iron droplets by slags containing iron oxide, and noticed that the rate was higher when the slag contained Fe_2O_3 than when it contained just FeO. They concluded that "slag oxygen potential, as given by the ferrous/ferric ratio, and the absolute concentration of ferric ions, had the most profound effect on the decarburization rate for a given carbon content." Unfortunately, they made no quantitative measurements of the reaction rate.

This study aimed therefore to determine what role ferric and ferrous iron in the slag played in the reaction rate. The goals of this part of the study included the following: (1) to determine quantitatively to what extent the overall reaction rate is higher when ferric cations are present in the slag; (2) to determine whether ferric cations are reduced before ferrous cations; (3) to understand the rate-limitation when only ferrous cations are present, and when both ferric cations and ferrous cations are present. It was hoped that

this study would explain why, in some cases, the decarburization of iron droplets does not proceed to completion.

1.3 Overview of experimental program

When the experimental program was started, experiments were performed following the method used in the study by Krishna Murthy et al.[8] In these initial experiments pieces of high-carbon iron were dropped into slags containing iron oxide. The reaction rate was measured by measuring the rate of pressure rise in a closed furnace. Soon it was apparent that this method would not work well for the present study, however.

Several problems with this type of experiment were identified. First, it was difficult to obtain a constant pressure reading. For many hours, at constant temperature in the "hot zone," the pressure in the furnace would rise. (The furnace that was used had a large volume of cool gas that could exchange with the gas in the hot zone; the pressure would rise slowly as the average temperature of the gas in the furnace rose.) Second, one could not use a very large metal mass. As the metal mass increased, the amount of CO evolved during the course of the reaction increased, so the peak pressure in the furnace increased; recall that the furnace was closed during the experiment. When the peak pressure rose too high, the furnace started leaking through various seals, and this made the pressure rise measurement inaccurate. A third problem with the initial experiments was that the pressure transducer's "zero point" drifted; this made it difficult to measure a low reaction

rate over an extended period of time, and most experiments were limited to about 30 minutes.

Another problem with the initial experiments was that the slag-metal area could not be determined accurately. Mulholland et al.[7] observed that a single droplet could break up into smaller droplets, and that the mass of a droplet could decrease during an experiment if the slag was highly oxidizing, as some iron would be oxidized. Finally, it was also realized that it would be difficult to perform "short-circuit" experiments with iron droplets in a slag bath. Several studies[7,10,11,12,8] have shown that, when the reaction rate is high, a droplet can be buoyed in the slag phase by the CO evolution. With the droplet "bouncing around" in the slag phase, it is not be possible to have continuous contact between the iron droplet and the short-circuit material.

A new type of experiment was devised. The most dramatic shift was to change from decarburization experiments to iron oxide reduction experiments. In the initial experiments, the iron oxide content remained the same, and the carbon content of the metal droplet decreased. In the new experiments, a much larger metal mass was used, so that it formed a continuous layer. In these new experiments, the carbon content remained the same, and the iron oxide content decreased. This change was made for two reasons. First, a short-circuit between the metal and the bulk slag phase would be straightforward since contact could be made continuously with the metal layer by simply penetrating the slag layer.

Second, the literature review had revealed that the most interesting effects were occurring as a result of the iron oxide content of the slag. By performing experiments in which both the total iron content of the slag and the ratio of ferric to ferrous cations changed, much more useful results would be obtained. In some experiments in this study, iron oxide pellets were added to a calcia-silica-alumina "base" slag to start the reaction. In other experiments in this study, crushed slag containing iron oxide was added to the molten high-carbon iron to start the reaction.

With the large metal mass used in the new experiments, the pressure-rise measurement had to be abandoned. In the new experiments, gas was passed continuously through the furnace, and two measurements were made continuously: (1) the inlet gas flow rate; and (2) the CO concentration in the outlet gas stream. The reaction rate is essentially the product of these two values.

Measuring the reaction rate by continuous monitoring of the gas composition had two important advantages over pressure-rise measurements. First, a large metal mass was possible. Second, much longer experiments, on the order of six hours, were possible; a low reaction rate could be measured over a much longer period than before since the gas analyzer's zero point was relatively stable.

1.4 Objectives of present study

This study comprises two parts (Figure 1). In the first part, the mechanism and rate of reduction of iron oxide from slag by carbon in iron were investigated. The author sought to test the following hypotheses in the first part of the study:

- the overall reaction rate is limited by the mass transport of iron cations;
- the reaction occurs in two stages, marked by the nature of the fluid flow conditions in the slag phase;
- the reaction occurs in two stages, marked by the dominant reduction reaction (i.e. ferric-to-ferrous or ferrous-to-metal);
- the ferric-to-ferrous reduction reaction is faster than the ferrous-to-metal reaction.

The first two hypotheses have been advanced previously in the literature; they were first proposed by Tarby and Philbrook[6]. The remaining two were developed by the author. based on an "electrochemical view" of the reduction of iron oxide from slag. According to this view, electrons supplied by the reaction in Equation (2) travel "through" the metal phase to another location on the slag-metal interface, where they are consumed by either the reduction of ferric or ferrous cations (Equations (3) and (4)). Wagner[13] was a proponent of this view, and several investigators[6,7,10,8] have discussed their results in terms of these reactions. However, there has been little experimental work aimed at studying these reactions individually.

The author wanted to know which reduction reaction occurs more quickly. It was expected that the ferric-to-ferrous reduction reaction would be faster since it requires only one electron and does not involve the transfer of chemical species from the slag phase to the metal phase. The ferrous-to-metal reduction reaction, on the other hand, requires two electrons and involves the transfer of iron from the slag phase to the metal phase.

The author wondered whether the reaction is occurring in two stages, marked by the dominant reduction reaction. During the first reaction stage, electrons produced by the oxidation of oxygen anions (Equation (2)) would be consumed by ferric cations at the slag-metal interface (Equation (3)), and the overall rate would be influenced by the rate of the ferric-to-ferrous reaction. During the second stage, electrons produced by the anodic reaction would be consumed at the slag-metal interface by ferrous cations (Equation (4)), and the overall reaction rate would be limited by the mass transport rate of ferrous cations.

In the second part of the study, the author sought to increase the rate of the reaction by electrochemical means. To this end, the "electrochemical nature" of the reduction of iron oxide under both unsteady- and steady-state conditions was studied. Unsteady-state conditions were obtained by allowing the iron oxide concentration to decrease over time. Steady-state conditions were obtained by oxidizing the slag at the gas-slag interface with CO_2 gas; in these experiments, the iron oxide concentration would remain constant over time. The author sought to test the following hypotheses in the second part of the study:

- the rate of reduction iron oxide from slag can be increased by short-circuiting the slag layer;
- the rate of reduction of iron oxide from slag can be increased by applying a voltage across the slag layer;
- the steady-state rate of decarburization of liquid iron is increased by applying a voltage across the slag layer.

It was expected that short-circuiting the slag layer would provide an electronic pathway from the metal bath to the bulk of the slag. If reduction reaction is limited by the mass transfer of iron cations, then this would increase the reaction rate. It was expected that applying a voltage would make this effect more dramatic.

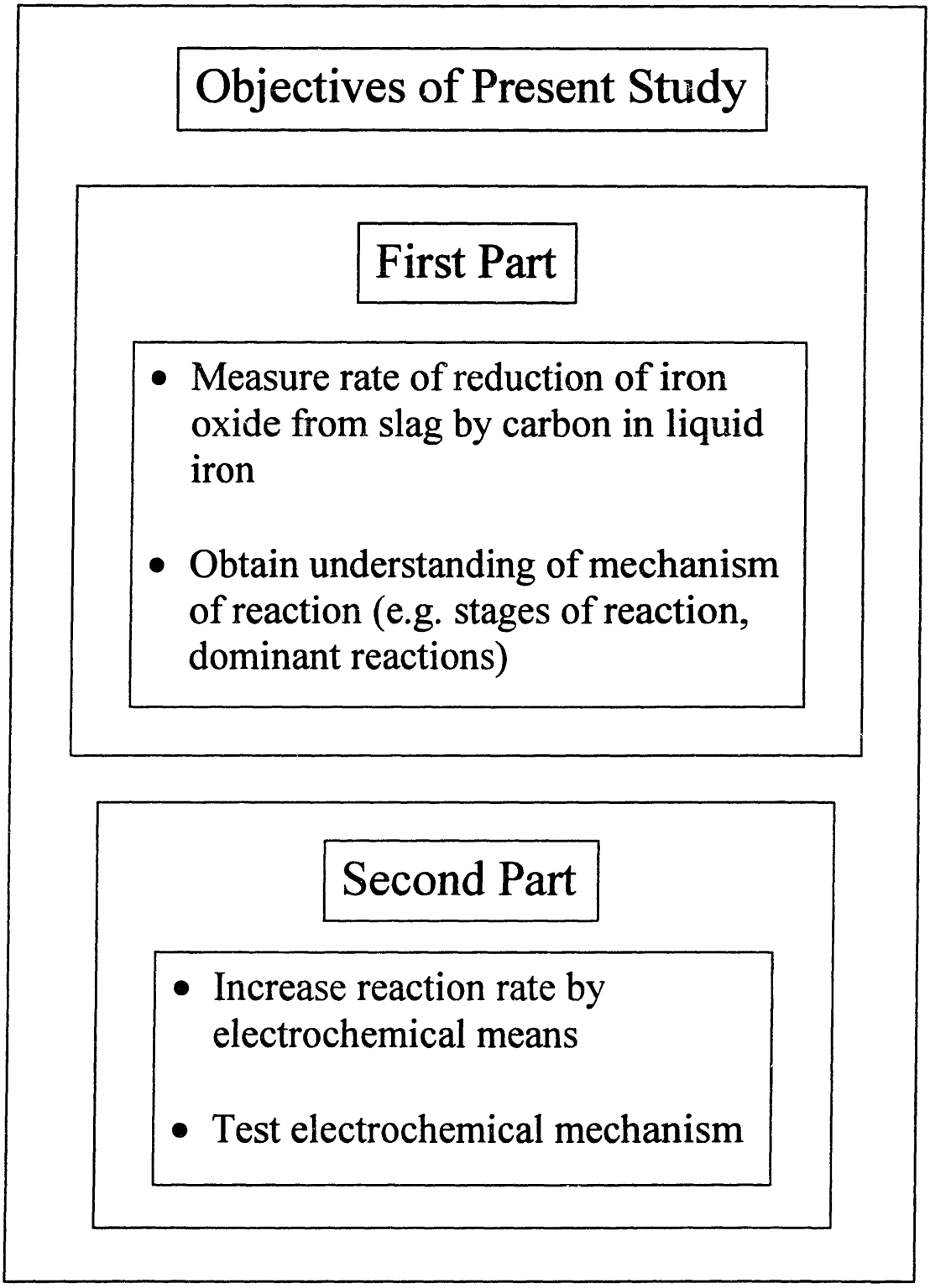

Figure 1. The present study is divided into two parts

1.5 Outline of the thesis

Following this Introduction, the literature on the reduction of iron oxide from slag by carbon in liquid iron is reviewed in Chapter 2. In Chapter 3, the experimental methods and procedures are discussed: design and construction of the furnace, procedure for a typical experiment, chemical analysis of metal and slag samples, and calculation of reaction rate from gas analyzer data. In Chapter 4, significant results of the study are presented. The first two sections of Chapter 4 cover the results from the first part of the study, in which the reaction rate and rate constant were determined. The remaining sections cover the short-circuit and applied-voltage experiments. In Chapter 5, the results of the study are discussed, and a model of the reaction rate is proposed. In addition, a physical explanation of the results of the short-circuit and applied-voltage experiments is offered. In Chapter 6, the conclusions of the thesis are given. Chapter 7 contains suggestions for further work. Appendices follow Chapter 7; these are referred to in the main body of the thesis.

Chapter 2. Literature Review

2.1 Literature on the reduction of iron oxide from slag by carbon in liquid iron

A number of studies have been performed to measure the rate of reduction of iron oxide from slag by carbon in liquid iron. In all the studies reviewed here, the slag and metal were in the form of molten layers. In addition, the iron oxide concentration fell significantly during these experiments, whereas the carbon concentration remained essentially unchanged. Therefore, this is a review of reaction rate measurements for "iron oxide reduction" experiments. Most of the studies have not reported the reaction rate, r, directly, but have instead reported the value of the "rate constant," k, in a power-law expression for the reaction rate, $r = kc^n$, where c is the bulk concentration of iron oxide in the slag phase, and n is the "order of reaction."

Philbrook and Kirkbride[5] found that their results obeyed a second-order rate expression. They reported that k was $5.8 \cdot 10^{-4}$ $\frac{\text{g FeO}}{\text{min cm}^2 \left[\text{wt\% FeO}\right]^2_{slag}}$ at 1430°C for a 47% CaO-38% SiO_2-15% Al_2O_3 base slag. One can calculate that the reaction rate is 0.03 $\frac{\text{mol O}}{\text{m}^2\,\text{s}}$ for 5 wt% FeO and 0.001 $\frac{\text{mol O}}{\text{m}^2\,\text{s}}$ for 1 wt% FeO.

Tarby and Philbrook[6] improved upon the study of Philbrook and Kirkbride. They found that their results could be modeled by a first-order rate expression. They reported that k was $9 \cdot 10^{-5} \frac{\text{g FeO}}{\text{min cm}^2 \left[\text{wt\% FeO}\right]_{slag}}$ at 1575°C for a 50% CaO-50% Al_2O_3 base slag, and $1 \cdot 10^{-3} \frac{\text{g FeO}}{\text{min cm}^2 \left[\text{wt\% FeO}\right]_{slag}}$ at 1575°C for a 50% CaO-8% SiO_2-42% Al_2O_3 base slag. One can calculate that the reaction rate is in the range $0.0002 - 0.01 \frac{\text{mol O}}{\text{m}^2\,\text{s}}$ if the concentration of FeO is in the range 1-5 wt%.

Sommerville et al.[14] also used first-order rate expression to model their results. One can estimate the value of k to be $1.6 \cdot 10^{-5} \frac{\text{m}}{\text{s}}$ from the graphical results they provide; temperature was 1380°C and the base slag was a 38% CaO-42% SiO_2-20% Al_2O_3. The calculated reaction rate is $0.02 \frac{\text{mol O}}{\text{m}^2\,\text{s}}$ for 3 wt% FeO and $0.007 \frac{\text{mol O}}{\text{m}^2\,\text{s}}$ for 1 wt% FeO. (It is assumed that the slag contains 1.63 moles per 100 grams of slag, and that the slag density is 2.5 g cm^{-3}.)

Upadhya et al.[15], working in the same laboratory as Sommerville et al., obtained similar results. One can estimate the value of k to be $2.2 \cdot 10^{-5} \frac{\text{m}}{\text{s}}$; the experimental conditions

were identical to those used by Sommerville et al. The calculated reaction rate is $0.02 \frac{\text{mol O}}{\text{m}^2\,\text{s}}$ for 2 wt% FeO and $0.009 \frac{\text{mol O}}{\text{m}^2\,\text{s}}$ for 1 wt% FeO.

Sato et al.[16] modeled their results with a second-order rate expression. They reported that k was $4 \cdot 10^{-4} \frac{\text{g FeO}}{\text{min cm}^2 \left[\text{wt\% FeO}\right]^2_{slag}}$ at 1520°C for a 53% CaO-36% SiO_2-11% Al_2O_3 base slag, and $1 \cdot 10^{-4} \frac{\text{g FeO}}{\text{min cm}^2 \left[\text{wt\% FeO}\right]^2_{slag}}$ at 1520°C for a 24% CaO-65% SiO_2-11% Al_2O_3 base slag. These results are similar to those obtained by Philbrook and Kirkbride. Sato et al. used an "integrating gas meter" to measure the volume of gas evolved as a function of time, and they assumed that all the gas produced was CO. The motivation for their study was to understand the "direct reduction" (i.e. direct smelting) process, and to determine optimal conditions for reduction of iron oxide from slag.

Wei et al.[17], using a first-order rate expression, gave the rate of decarburization of the metal bath in units of wt% C per minute. In their experiments, both the concentration of carbon in liquid iron, and the concentration of iron oxide in slag, fell significantly. The initial rate of decarburization was reported for FeO concentrations in the range 10-20 wt%. The slag and metal were stirred mechanically with an alumina stirring rod at 200 revolutions per minute. The reported rates were in the range $1 \cdot 10^{-3}$ to $6 \cdot 10^{-2} \frac{\left[\text{wt\% C}\right]_{metal}}{\text{min}}$ at 1300 for a 38% CaO-41% SiO_2-21% Li_2O base slag. The

calculated rates are in the range $0.003-0.02\ \frac{\text{mol O}}{\text{m}^2\,\text{s}}$. The following values are used in the calculation: 300 g for the metal mass, and 4.0 cm for the diameter of the crucible.)

Krishna Murthy et al.[18] found that their results could be modeled with a first-order rate expression. They reported that k was $1.2\cdot10^{-5}\ \frac{\text{m}}{\text{s}}$ at 1450°C for a 43% CaO-38% SiO_2-11% Al_2O_3 base slag. The calculated rate is $0.04\ \frac{\text{mol O}}{\text{m}^2\,\text{s}}$ for 8.4 wt% FeO, and $0.01\ \frac{\text{mol O}}{\text{m}^2\,\text{s}}$ for 2 wt% FeO.

Paramguru et al.[19] also used a first-order rate expression to model their results. They reported that k varied with concentration of FeO in the slag. For experiments at 1400°C with a 50% CaO-50% SiO_2 base slag, k was in the range $1.0\cdot10^{-5}-9.2\cdot10^{-5}\ \frac{\text{m}}{\text{s}}$. The calculated rate is $0.04\ \frac{\text{mol O}}{\text{m}^2\,\text{s}}$ for 10 wt% FeO.

Most investigators have used a first-order rate expression. The results of several investigators show that the order of reaction increases at low concentrations of iron oxide in the slag. Table I summarizes results from the studies discussed in this section; results from the present study are also included. Table II gives details on the experimental parameters used in previous studies.

Table I. Literature on the rate of reduction of iron oxide from slag by Fe-C

Investigators	Reaction rate observed (mol O m^{-2} s^{-1})	Order of Reaction	Rate Constant
Philbrook and Kirkbride[5]	0.001 to 0.03	2	$8x10^{-9}$ m^4 mol^{-1} s^{-1}
Tarby and Philbrook[6]	0.0002 to 0.01	>1 initially 1 near completion	$5x10^{-7}$ to $6x10^{-6}$ m s^{-1}
Sommerville et al.[14]	0.007 to 0.02	1	$2x10^{-5}$ m s^{-1}
Upadhya et al.[15]	0.009 to 0.02	1 >1 near completion	$2x10^{-5}$ m s^{-1}
Sato et al.[16]	0.006 to 9	2 >2 near completion	$1x10^{-9}$ and $2x10^{-8}$ m^4 mol^{-1} s^{-1}
Wei et al.[17]	0.003 to 0.2	N.A.	N. A.
Krishna Murthy et al.[18]	0.01 to 0.04	1	$1x10^{-5}$ m s^{-1}
Paramguru et al.[19]	0.04 to 2	1	$1x10^{-5}$ to $9x10^{-5}$ m s^{-1}
Present Study	0.001 to 0.1	1 >1 near completion	$1x10^{-6}$ to $1x10^{-5}$ m s^{-1}

Table II. Experimental parameters in previous studies

Investigators	Measurement	Crucible	T (°C)	A_{s-m} (cm^2)	m_{slag} (g)	m_{metal} (g)	Base slag $CaO-SiO_2-Al_2O_3$	Initial iron oxide conc.	Length of expt. (min.)	Notes
Philbrook and Kirkbride[5]	slag sampling, analysis for total iron	graphite	1430, 1570	18	65 or 100	300	47-38-15	0.32-4.98% 'FeO'	15-100	Base slag composition made to simulate BF slag
Tarby and Philbrook[6]	slag sampling, analysis for total iron	graphite	1500, 1575	32	100	400	50-0-50 50-8-42 51-40-9	<5% FeO	60	FeO added to molten base slag
Sommerville et al.[14]; Upadhya et al.[15]	pressure rise	alumina (metal), steel (slag)	1380, 1410	6.4	30	30	38-42-20 T_m= 1265°C	1.5-3.2% FeO	160	Base slag composition made to simulate BF slag
Sato et al.[16]	volume of gas evolved	graphite and alumina	1320-1620; mainly 1520	24	57	1500	24-66-11 44-45-11 53-36-11 58-32-11	5-50% FeO; mainly 30% FeO	30	rate highest for CaO/SiO_2 = 1.5;
Wei et al.[17]	slag sampling; analysis for total iron	alumina	1300	13	33-37	300	38-41-0 21% Li_2O	10-20% FeO		mechanical stirring with alumina rod
Krishna Murthy et al.[18]	pressure rise	alumina	1450	27	10-90	400	47-41-12	8.4% FeO	40-80	
Paramguru et al.[19]	weight loss (thermo-gravimetric apparatus)	graphite	1200-1400	0.8	2	20	33-66-0 50-50-0 60-40-0 66-33-0	10-60% FeO	25	rate highest for CaO/SiO_2 = 1.5

2.2 Literature on electrochemical aspects of slag-metal reactions

As discussed in the Chapter 1, Krishna Murthy et al.[8] reported that the rate of decarburization of an Fe-C droplet by slag containing FeO is increased by lining the crucible with molybdenum foil. Several investigators have used metal wires to provide "pathways" for the electrons produced in anodic reactions. In one study, Pal et al.[20] showed that penetrating a lead oxide-silica slag with iridium wires increased the rate of oxidation of liquid lead by oxygen in the gas phase.

If one metal wire is connected to the metal bath, a second wire is connected to the slag layer, and they are connected through an external circuit, then the "short-circuit" current should be measurable. In a study by Grimble et al.[21], silica in slag was simultaneously reduced by a carbon rod dipped in the slag, and by a carbon-saturated iron bath; current was measured through an external circuit that connected the carbon rod to the liquid iron bath.

A direct-current power supply can be attached across two wires, where one wire is dipped in the slag and one is dipped in the metal phase. A voltage can then be applied across the slag layer. The applied voltage should result in an increase in the electrochemical current, and an increase in the observed reaction rate. McLean et al.[22], in a study on the desulfurization of steel, applied a voltage across the slag layer, and observed an increase in the rate of desulfurization. They used a transferred-arc DC plasma as the anode, and

the cathode was the metal bath; electrical contact was made with the bath through an electronically conducting hearth.

Chapter 3. Experimental Apparatus and Procedures

3.1 Design and construction of furnace and gas system

The experiments were conducted in an induction furnace (Figure 2). The "outer furnace tube" is made of mullite, and has a diameter of 22.9 cm (9 in.) and a length of 91.4 cm (36 in.). The outer furnace tube rests on the bottom plate, which is made of brass and is supported by a frame (not pictured). Everything inside the outer furnace tube rests on a steel plate, which is supported by six steel compression springs. On top of the steel plate are alumina bricks. A layer of silica-alumina fiber insulation is placed above the bricks, followed by several layers of graphite felt insulation. The susceptor, made of graphite, rests on this graphite felt. The diameter of the susceptor is 17.1 cm (6.75 in.) and its length is 45.7 cm (18 in.).

Graphite felt is wrapped around the susceptor, and is also placed above the susceptor. A one-end closed alumina tube, the "inner furnace tube," is placed inside the susceptor, and rests on graphite felt. Alumina board-like insulation is placed in the bottom of the inner furnace tube, and some alumina-silica, fiber-like insulation is placed on top of this. For each experiment, an alumina crucible was used, and this was placed in the inner furnace tube on the fiber insulation. Figure 2 shows a crucible that is just a bit smaller in diameter than the inner furnace tube. Although this was the case in some experiments, in

a number of experiments, the crucible was not so large as pictured in Figure 2, and there was a significant space between the crucible and the inner furnace tube.

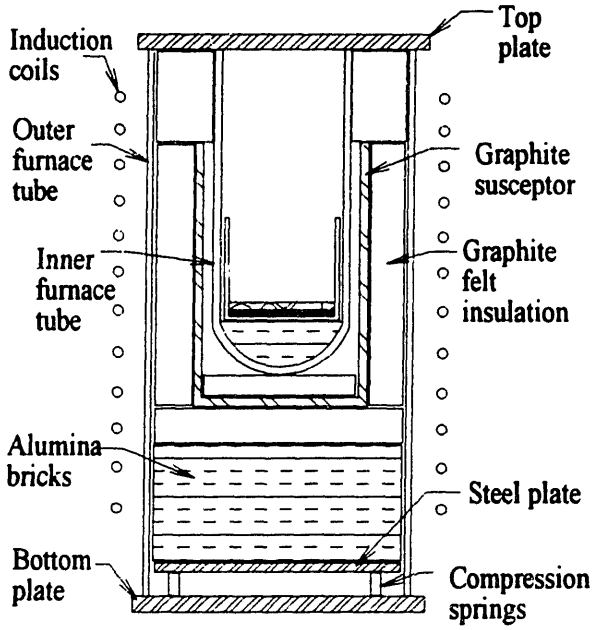

Figure 2. An induction furnace was used in this study

Before the top plate, which was made of stainless steel, was put on the furnace, the inner furnace tube extended above the top of the outer furnace tube by about 3 cm. Silica-alumina fiber insulation was placed inside the inner furnace tube above the crucible, and a silicone rubber gasket was positioned on top of the inner furnace tube. Then, the top plate was lowered down onto the top of the inner furnace tube. The top plate was secured to the top of the outer and inner furnace tubes by a set of bolts that connected the top plate to a frame (not pictured) that was built around the outer furnace tube.

When the top plate was bolted down, the compression springs positioned under the bottom plate applied adequate upward force to form a good seal at three lines of contact: (1) the outer tube with the bottom plate; (2) the outer tube with the top plate; and (3) the inner tube with the top plate. Silicone rubber gaskets with a thickness of 0.64 cm (0.25 in.) were used between the furnace tubes and the top and bottom plates; the hardness of the rubber was 30 durometer.

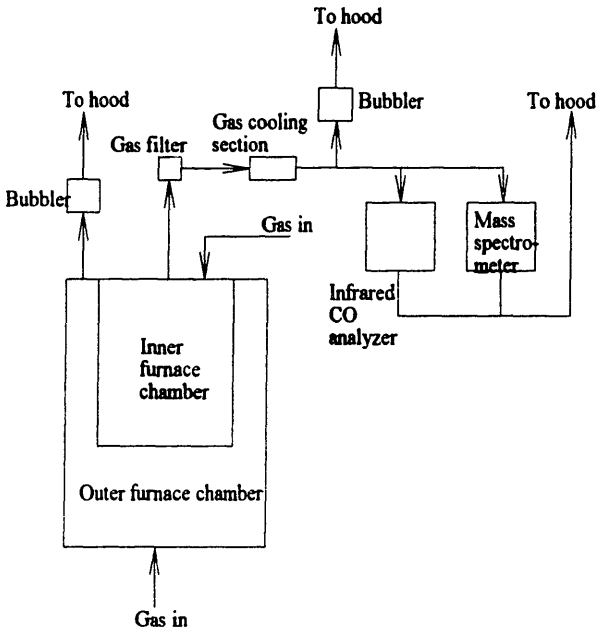

Figure 3. Gas analysis was used to determine the reaction rate

A thermocouple protection tube, pyrometer sight tube, gas inlet tube, gas outlet tube, and sampling tube passed through stainless-steel fittings in the top plate. (Holes were made in the fiber insulation placed above the crucible to allow these to pass through.) In some

experiments electrodes also passed through the top plate. A gas seal was maintained around these tubes by silicone rubber gaskets inside the fittings.

The furnace is composed of two "chambers" (Figure 3). The outer chamber is the space between the outer and inner furnace tubes, while the inner chamber is the space inside the inner furnace tube. During experiments argon was passed through both the inner and outer furnace chambers. The flow rate of gas to the inner chamber was measured before it entered the inner furnace tube. The gas exiting the inner furnace chamber was filtered and cooled. Some of the outlet gas was passed through an infrared CO analyzer (ANARAD Model AR-411 Single-Gas Portable Gas Analyzer), and some through a mass spectrometer (AMETEK M200 Series Quadrupole Gas Analyzer).

3.2 Procedure for a typical experiment

In a typical experiment, a mass of iron-carbon alloy was melted in an argon atmosphere and the temperature was stabilized at the desired temperature for the experiment (in the range 1400-1600°C). The temperature was measured with a type-B thermocouple and also with a two-color pyrometer (IRCON MODLINE R Series Two-Color Pyrometer, Model R-20C05-0-1-0-31-0/642). Then, the CO analyzer was calibrated by passing a certified Ar-10 vol% CO gas mixture through the system. The Fe-C alloy initially contained 5 wt% C. Analysis of metal samples from the end of experiments showed that

the carbon concentration had not decreased significantly. The mass of metal used in each experiment was in the range 500-700 g.

Table III. Description of experiments in first part of study

Experiment #	Slag-metal area (cm^2)	Slag mass (g)	Total iron (weight percent)	Ferrous iron (weight percent)	Temperature (°C)
1	30.2	59.0	5.00	2.22	1400
2	30.2	116	5.00	2.22	1400
3	52.8	213	5.00	2.22	1400
4	52.8	213	5.00	2.22	1400
5	49.0	330	5.00	2.22	1400
6	49.0	302	5.00	2.22	1600
7	49.0	300	5.01	2.66	1400
9	49.0	200	16.1	8.05	1400
10	49.0	300	5.01	2.66	1400
16	49.0	300	5.01	2.66	1600
17	49.0	300	16.1	8.05	1600
18	49.0	300	16.1	8.05	1600
19	49.0	300	16.1	8.05	1500

For experiments in the first part of the study, the next step was to drop a mass of crushed slag containing iron oxide through a port in the top of the furnace. The slag dropped through an alumina "sampling" tube that had an outside diameter of 2.54 cm (1 in.), and fell into the crucible, landing on top of the molten metal layer. The slag containing iron oxide was made ahead of time in another induction furnace by adding Fe_2O_3 powder to molten "base slag." The base slag composition was 48 wt% CaO, 40 wt% SiO_2, and 12 wt% Al_2O_3, and the slag initially contained 5 or 16 wt% total iron (in the form of ferrous and ferric cations). The mass of slag added in an experiment was in the range 59-330 grams. Details of the parameters for the experiments in the first part of the study are

given in Table III. Note that in all the experiments about half of the iron oxide was ferric, and half was ferrous.

Table IV. Description of experiments in second part of study

Experiment description	Inner furnace tube volume (L)	Slag-metal area (cm^2)	Metal mass (g)	Metal depth* (cm)	Slag mass (g)	Slag depth** (cm)	Atmos-phere
Short-circuit #1	3.79	52.8	605	1.7	200	1.5	Argon
Short-circuit #2	3.79	52.8	772	2.2	150	1.1	Argon
Short-circuit #3	3.79	52.8	519	1.4	289	2.2	Argon
Decarburization #1	3.79	52.8	657	1.8	296	2.2	Ar-6% CO_2
Decarburization #2 (with electrolysis)	3.79	52.8	519	1.4	289	2.2	Ar-6% CO_2
Decarburization #3 (with plasma electrolysis)	3.79	52.8	624	1.7	476	3.6	Ar-5% CO_2
Reduction #1 (with electrolysis)	3.79	52.8	519	1.4	289	2.2	Argon
Reduction #2 (with plasma electrolysis)	4.74	52.8	515	1.4	167	1.3	Argon
Reduction #3 (with plasma electrolysis)	4.74	52.8	579	1.6	177	1.3	Argon

*Depth of liquid metal layer calculated by assuming that the density of the Fe-C metal is 6.8 g cm^{-3}.
**Depth of slag layer calculated by assuming that the density of the slag is 2.5 g cm^{-3}.

Two types of experiments were done in the second part of the study. In the first type, base slag and Fe-C metal were placed together in the crucible and melted; pure iron oxide was later added to the slag during the experiment. In the second type of experiments, the Fe-C metal was melted by itself, and during the experiment slag containing iron oxide

was added to the crucible (as discussed above for experiments in the first part of the study). The mass of slag used in each experiment was in the range 150-500 g.

Three power supplies were used during the second part of the study to apply a voltage between the metal bath and a second electrode. The second electrode was either dipped in the slag layer or held above the slag layer. For decarburization experiment #2 and reduction experiment #1, a 10A-20VDC Hewlett-Packard power supply (Model HP 6033A) was used. For decarburization experiment #3, a 600A-44VDC Thermal Arc welding power supply (Model 600 GMS) was used. For reduction experiments #2 through #4, a 100A-100VDC Electronic Measurements (EMI) power supply (Model TCR100T100-4-OV) was used. Details of the parameters for experiments in the second part of this study are included in Table IV. Some further details on the experimental procedures used in specific experiments are included in the Results section.

3.3 Analysis of metal and slag samples

The metal samples were analyzed for carbon concentration by the analytical lab of the LECO Corporation (St. Joseph, MI). In some experiments, slag samples were taken, and these were analyzed by the author by titrating with a potassium dichromate solution[23,24,25]. Each slag sample was ground to pass an 80-mesh sieve using a porcelain mortar and pestle. The sample was then divided into two parts. One part was analyzed for ferrous iron, and the other was analyzed for total iron (i.e. for the sum of ferrous and

ferric iron, in the absence of metallic iron); the amount of ferric iron was then calculated by difference.

To analyze a sample for ferrous iron, the following procedure was used. A sample of about 0.5 gram of slag was weighed into a 250-ml filter flask. Then 50 ml deionized water and 50 ml concentrated hydrochloric acid (HCl) were added. The flask was heated under reflux and an argon atmosphere to incipient boiling on an hot plate (typically about 15 minutes). The flask was removed from the hot plate, and then 5 ml of concentrated HCl was added. The solution was transferred quantitatively to a 400-ml beaker, and then diluted to 200 ml with deionized water. Next 5 ml saturated mercuric chloride solution was added. The solution was stirred for a few seconds with a glass stirring rod, and then 20 ml of a solution of sulfuric and phosphoric acids was added. Eight drops of diphenylamine indicator solution were added, and then the sample was titrated with a potassium dichromate solution to a purple endpoint.

To analyze a sample for total iron, a similar procedure was followed. A sample of about 0.5 gram of slag was weighed into a 150-ml beaker. Then 50 ml deionized water and 50 ml concentrated hydrochloric acid were added. The beaker was heated under reflux and an air atmosphere to incipient boiling on a hot plate (typically about 15 minutes). The beaker was removed from the hot plate, and then a stannous chloride solution was added, one drop at a time, to a colorless endpoint. Next, 5 ml of concentrated HCl was added, and the solution was transferred quantitatively to a 400-ml beaker. The solution was

diluted to 200 ml with deionized water, and then 5 ml saturated mercuric chloride solution was added. The solution was stirred for one minute with a glass stirring rod, and then 20 ml of a solution of sulfuric and phosphoric acids was added. Eight drops of diphenylamine indicator solution were added, and then the sample was titrated with a potassium dichromate solution to a purple endpoint.

The saturated mercuric chloride solution is available for purchase. The solution of sulfuric and phosphoric acids was made by filling a 1-L volumetric flask with about 400 ml of deionized water, then adding 125 ml concentrated sulfuric acid and 200 ml concentrated phosphoric acid, and finally diluting with deionized water to 1 L. The diphenylamine solution was prepared by dissolving 1.0 gram of the reagent in 100 ml of concentrated sulfuric acid. The potassium dichromate solution was prepared by weighing the desired amount of dried potassium dichromate ($K_2Cr_2O_7$) into a 250-ml beaker and then adding 100 ml deionized water. The solution was stirred to completely dissolve the $K_2Cr_2O_7$, and then it was transferred to a 500-ml volumetric flask. Deionized water was added to dilute to the mark, and the solution was transferred to a 500-ml bottle with a plastic screw cap for storage. The normality of the solution was calculated using the following formula:

$$N\left[\frac{\text{eq}}{\text{L}}\right] = \frac{x[\text{g}]}{\left(49.032\left[\frac{\text{g}}{\text{eq}}\right]\right)(0.5[\text{L}])} \tag{5}$$

where x was the mass of $K_2Cr_2O_7$ used. The stannous chloride solution was prepared by weighing about 36 grams of stannous chloride ($SnCl_2.H_2O$) into a 400-ml beaker. Next,

300 ml of hot, concentrated HCl was added. After all the stannous chloride was dissolved, the solution was transferred to a 500-ml volumetric flask and diluted with deionized water to the mark. The solution was then transferred to a 500-ml Erlenmeyer flask; the flask was stored with a rubber stopper in place to prevent exposure of the solution to air.

3.4 Analysis of gas composition data

The reaction rate "in terms of CO," r_{CO}, was calculated from measurements of the inlet gas flow rate and the CO concentration in the outlet gas stream (i.e. the gas coming out of the inner furnace chamber), using the following formula:

$$r_{CO}\left[\text{mol}/\text{m}^2\text{s}\right] = \left(1.08 \times 10^{-5}\right)\frac{Q_{inlet}(\%CO)}{A} \tag{6}$$

The inlet flow rate, Q_{inlet}, is in units of standard liters per minute of nitrogen (i.e. the flow meter is calibrated for nitrogen), the concentration of CO in the outlet gas stream, $\%CO$, is in mole percent, and the slag-metal interfacial area, A, is in square meters. Data from the mass spectrometer showed the concentration of carbon dioxide (CO_2) in the outlet gas stream was negligible; therefore the reaction rate "in terms of CO," measured in this study, is equal to the reaction rate in "terms of oxygen."

$$r_{CO} = r_O \tag{7}$$

That is, there is a one-to-one correspondence between the reaction rate in units of moles of CO per unit area per unit time, and moles of oxygen per unit area per unit time. The

concentration of "oxygen associated with iron cations" in the slag phase was calculated with the following formula:

$$[wt.\%O]_{slag} = 0.287\left(\left[wt.\%Fe^{2+}\right]_{slag} + 1.5\left[wt.\%Fe^{3+}\right]_{slag}\right) \quad (8)$$

The value of $[wt.\%O]_{slag}$ is a measure of the "oxidizing power" of the slag. (See Appendix A. Relationships between measures of iron oxide concentration.)

Chapter 4. Results

4.1 Measurements of rate of reduction of iron oxide

Figure 4 shows the reaction rate as a function of time for a typical experiment. This plot is essentially the "raw" data obtained in a typical experiment from the gas analysis. The trace is not smooth, since the CO concentration in the outlet gas fluctuated when the reaction rate was high; these fluctuations were the result of individual CO bubbles bursting through the slag layer, or of the foamed slag layer collapsing periodically. (See Appendix G. Contact time.) The trace has been "smoothed" by an averaging procedure, so the frequency of the peaks in Figure 4 do not correspond to the frequency of bubbles bursting.

The reaction rate rises rapidly after the slag is added to the crucible. As iron oxide is reduced, the reaction rate decreases, and after several hours, the reaction rate is nearly zero. Final slag analysis showed, however, that the slag still contained iron oxide (Table V). Equilibrium calculations for the reduction of ferrous oxide from slag by carbon in liquid iron show that the concentration of ferrous cations in the slag should be close to zero when equilibrium is achieved. (See Appendix B. Concentration of FeO in slag in equilibrium with liquid Fe-C.)

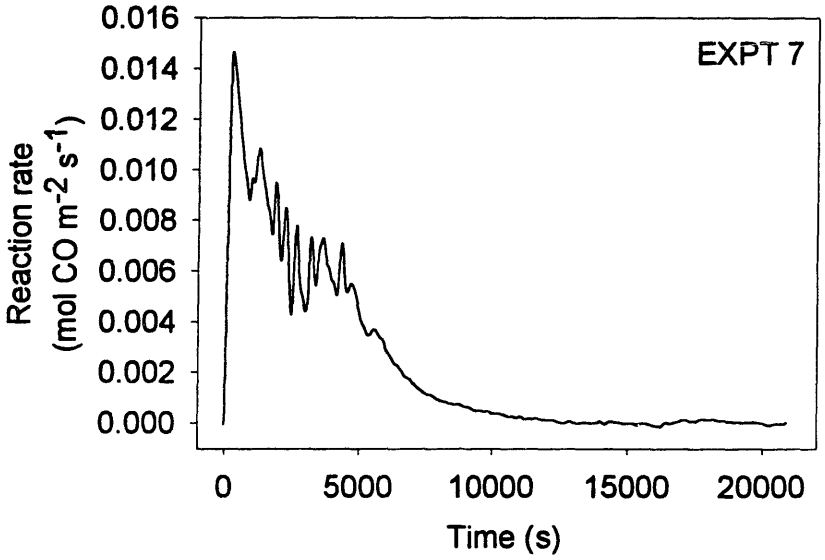

Figure 4. Reaction rate *vs.* time for a typical experiment

Table V. Results of final slag analysis for several experiments

Experiment #	Total iron (weight percent)	Ferrous iron (weight percent)	$[wt.\%O]_{slag}$
1	0.85	0.77	0.26
2	0.59	0.51	0.18
3	0.67	0.65	0.20
4	0.65	0.62	0.19
10	0.66	0.70	0.20

Figure 5 shows the reaction rate in terms of CO as a function of $[wt.\%O]_{slag}$ for several experiments at 1400°C. The value of $[wt.\%O]_{slag}$ at time t was calculated by integrating

the reaction rate; the initial value of $[wt.\%O]_{slag}$ was calculated from the data in Table III using Equation (8). The following equation was used for the integration:

$$[wt.\%O(t)]_{slag} = [wt.\%O(t_o)]_{slag} - \frac{1600 A_{s-m}}{m_s} \int_{t'=t_o}^{t'=t} r_{CO}(t')\,dt' \qquad (9)$$

where r_{CO} is the reaction rate in terms of CO (i.e. moles of CO per unit area per unit time), m_s is the mass of slag, and $A_{s\text{-}m}$ is the slag-metal interfacial area.

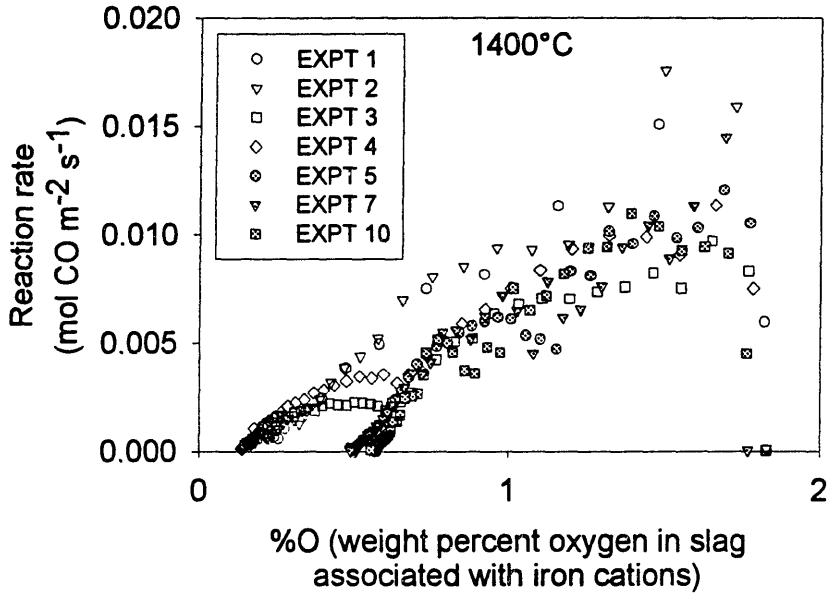

Figure 5. Reaction rate in terms of CO at 1400°C

The data in Figure 5 shows that the reaction rate falls as $[wt.\%O]_{slag}$ decreases. (The reaction rate is low at the initial value of $[wt.\%O]_{slag}$ since the slag initially is solid and

not reactive.) The reaction rate should be zero when equilibrium is achieved (i.e. when $[wt.\%O]_{slag}$ is nearly equal to zero). However, equilibrium is not achieved, and the reaction rate goes to zero at a value of $[wt.\%O]_{slag}$ greater than zero; chemical analysis of the slag showed that the final $[wt.\%O]_{slag}$ was typically in the range 0.2-0.3 (Table V). The final value of $[wt.\%O]_{slag}$ calculated from the gas analysis data was sensitive to the calibration of the gas analyzer, and was typically in the range 0.2-0.6.

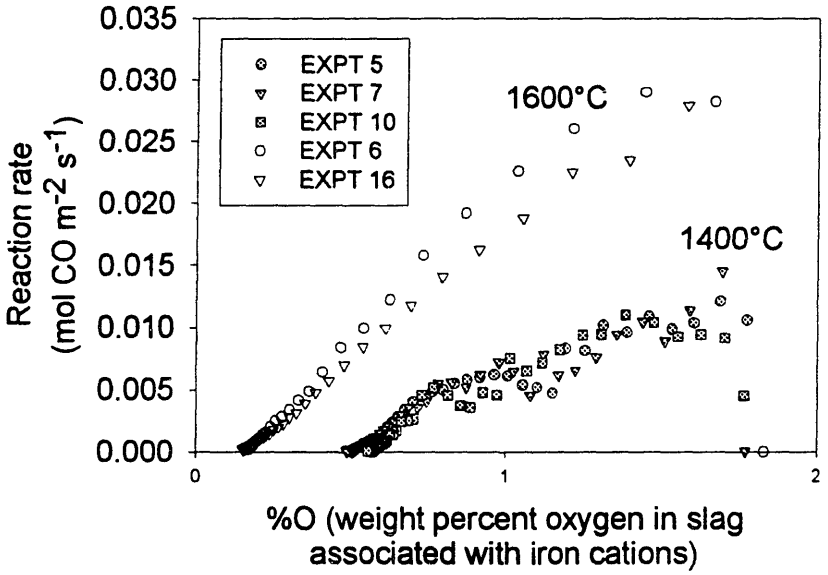

Figure 6. Reaction rate in terms of CO at 1400 and 1600°C

Figure 6 shows the reaction rate at 1400 and 1600°C for experiments in which the slag mass was approximately 300 grams, and in which the initial total iron content was about

5 wt%. The reaction rate is higher at 1600°C. Note that this behavior is expected whether the rate-controlling mechanism is a mass transfer step or a chemical reaction step. The activation energy for the reaction can be calculated from the reaction rate at two temperatures:

$$E_A = \frac{RT_1T_2}{T_2 - T_1} \ln\left(\frac{r_2}{r_1}\right) \tag{10}$$

Comparison of the reaction rates at 1400 and 1600°C for $[wt.\%O]_{slag} \cong 1.7$ yields an activation energy of approximately 120 kJ mol^{-1}.

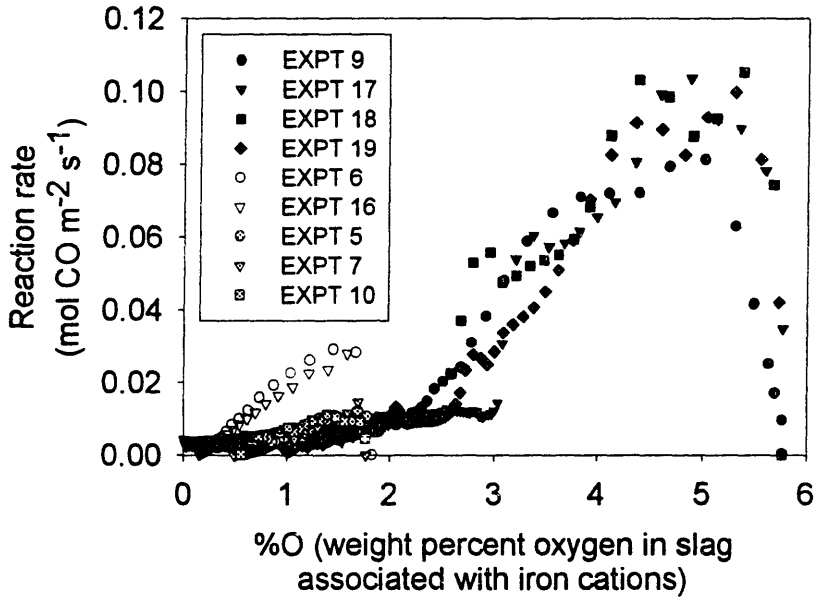

Figure 7. Reaction rate in terms of CO for slag initially containing 5 or 16 wt% Fe

Experiments were also conducted using slag initially containing 16 wt% total iron; these were conducted over the temperature range 1400-1600°C. Data from these experiments is plotted in Figure 7 along with rate data for experiments in which the slag initially contained 5 wt% total iron. Note that the reaction rate is relatively insensitive to temperature at high concentrations; comparison of reaction rates for experiments 9 and 17 (at 1400 and 1600°C) for $[wt.\%O]_{slag} \cong 5$ yields an activation energy of approximately 35 kJ mol^{-1}. For experiments 9 and 17 at $[wt.\%O]_{slag} \cong 1.7$, the activation energy is 110 kJ mol^{-1}. (The rates for these two experiments are the following: 0.0054 mol CO m^{-2} s^{-1} for experiment 9 at 1400°C; 0.012 mol CO m^{-2} s^{-1} for experiment 17 at 1600°C.)

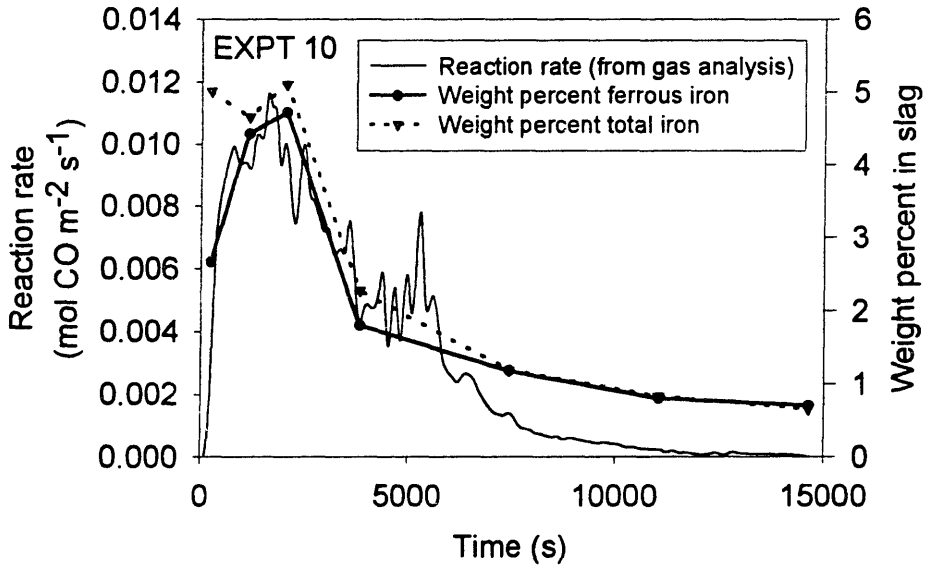

Figure 8. Simultaneous gas analysis and slag analysis data from one experiment

The data in Figure 7 also show that the reaction rate at $[wt.\%O]_{slag} \cong 1.7$ is lower in the case of the experiments in which the slag initially contained 16 wt% Fe. It is proposed that the reason for this difference is that in the case of experiments 5, 7, 10, 6, and 16, there is ferric iron present in the slag when $[wt.\%O]_{slag} \cong 1.7$, whereas in the case of experiments 9, 17, 18, and 19, nearly all iron in the slag is ferrous at this point.

Several experiments were conducted in which slag sampling and gas analysis were performed simultaneously. The results for one of these experiments are shown in Figure 8. It can be seen that ferrous iron in the slag, initially about half of the total iron, rises rapidly, while the total iron remains nearly constant. Therefore, the ferric cations are reduced to ferrous cations during the initial period of reaction according to the reaction in Equation (3).

4.2 Rate constant and mass transfer coefficient measurements

In a first-order rate expression, the reaction rate, r, is directly proportional to the concentration (of a reactant), c,

$$r\left[\frac{\text{mol}}{\text{m}^2\,\text{s}}\right] = k\left[\frac{\text{m}}{\text{s}}\right]\cdot c\left[\frac{\text{mol}}{\text{m}^3}\right] \tag{11}$$

and the proportionality constant, k, is called the rate constant. (SI units for the quantities are enclosed in square brackets.) The reaction rate can be written in terms of the derivative of the concentration with respect to time.

$$r\left[\frac{\text{mol}}{\text{m}^2\,\text{s}}\right] = -\frac{V\left[\text{m}^3\right]}{A\left[\text{m}^2\right]}\cdot\frac{dc}{dt}\left[\frac{\text{mol}}{\text{m}^3\,\text{s}}\right] \tag{12}$$

Substituting Equation (12) into Equation (11) and integrating, one obtains the following equation:

$$k(t-t_o) = -\frac{V}{A}\ln\left(\frac{c(t)}{c(t_o)}\right) \tag{13}$$

For the reduction of iron oxide from slag by carbon in liquid iron under conditions where the concentration of carbon is constant, the reaction rate depends on the concentration of iron oxide in the slag. In this study, both ferric and ferrous cations were present in the slag initially, and the two concentrations have been used to calculate the "weight percentage of oxygen in the slag associated with iron cations," $[wt.\%O]_{slag}$, using

Equation (8). If the concentration is given in terms of $[wt.\%O]_{slag}$, then Equation (13) can be written as

$$-k(t-t_o)=\frac{V_{slag}}{A_{slag-metal}}\ln\left\{\frac{[wt.\%O(t)]_{slag}}{[wt.\%O(t_o)]_{slag}}\right\}, \tag{14}$$

and a plot of the quantity on the right-hand side of Equation (14) versus time has a slope equal to $-k$.

Figure 9 shows that the rate constant at 1600°C is higher than that at 1400°C. Also, the rate constant decreases with time; this behavior is not expected for a chemical rate constant. The observation that the rate constant decreases with time supports the hypothesis that the reaction rate is limited by mass transfer in the slag phase. If the reaction rate is indeed limited by mass transfer (of iron oxide) in the slag phase, then the observed rate constant, k, is a mass transfer coefficient, and the reaction rate is proportional to the difference in concentration (of iron oxide) between the bulk slag and the slag at the slag-metal interface.

$$r=k_D\left(c_{bulk}-c_{interface}\right) \tag{15}$$

The mass transfer coefficient is expected to decrease as the reaction rate decreases, since the rate of CO evolution decreases, and the slag is less vigorously stirred. Interpreted in this light, the data in Figure 9 show that the mass transfer coefficient decreases with time.

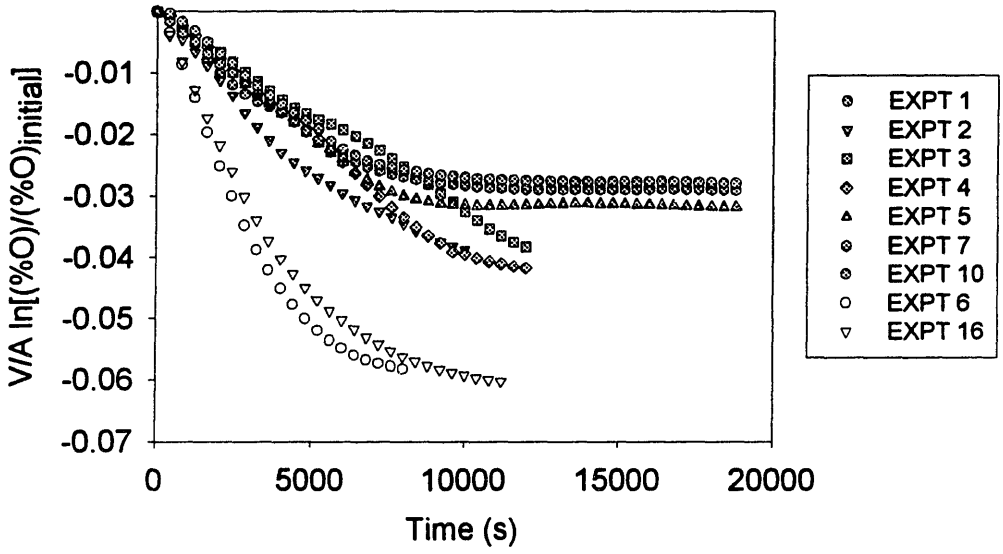

Figure 9. Plot of V/A $\ln[(\%O)/(\%O)_{initial}]$ *vs.* time

In Figure 10 the quantity on the right-hand side of Equation (14) is plotted versus time for the experiments in which the slag initially contained 16 wt% total iron. Recall that the rate of reaction was very high initially for these experiments (Figure 7). The data in Figure 10 show that the rate constant was not any higher for these experiments than it was for experiments 6 and 16 (conducted at 1600°C with slag initially containing 5 wt% total iron). Note that the slope of the traces for experiments 17 and 18 increase at long times, because in these experiments the calculated final value of $[wt.\%O]_{slag}$ was close to zero; the quantity plotted on the ordinate therefore tends toward negative infinity at long times.

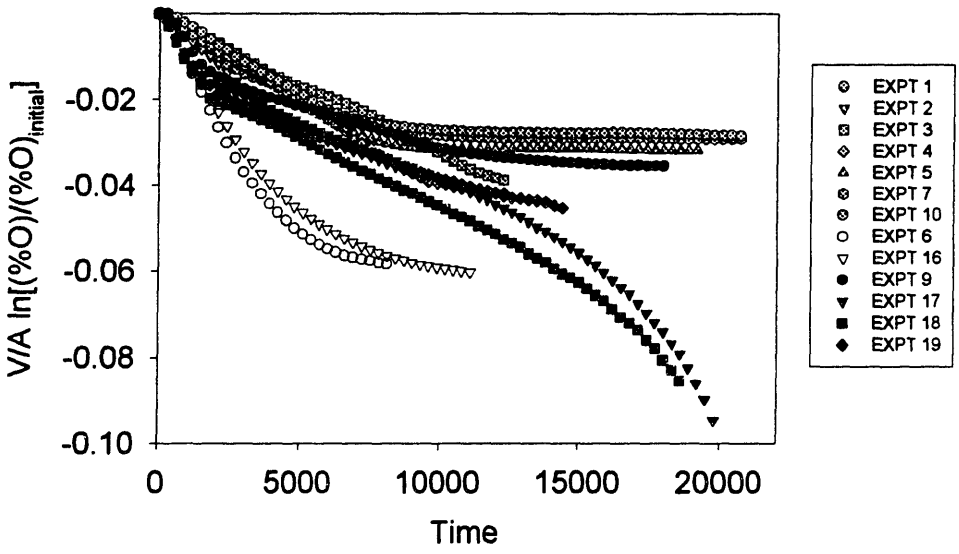

Figure 10. Plot of V/A $\ln[(\%O)/(\%O)_{initial}]$ *vs.* time

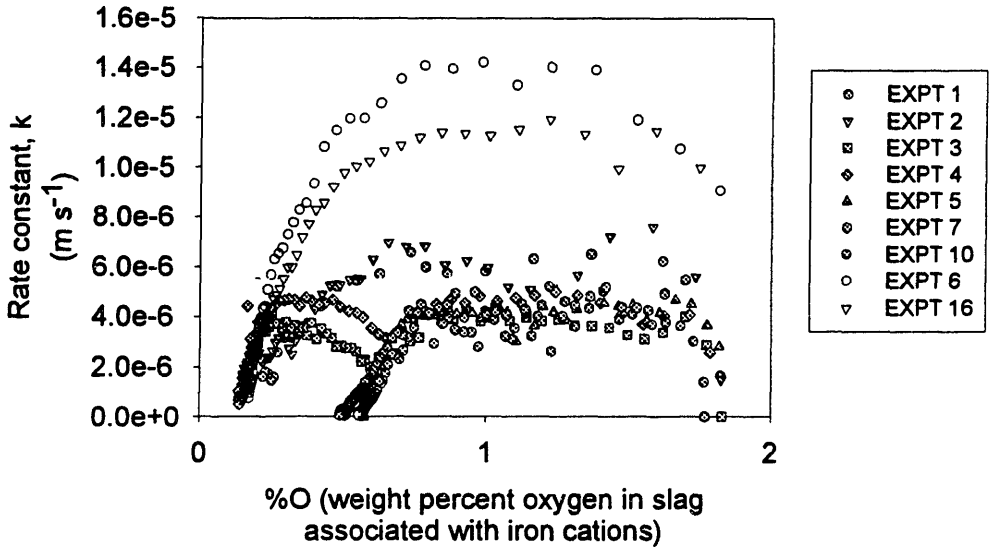

Figure 11. Plot of the rate constant *vs.* concentration at 1400 and 1600°C

The rate constant can also be calculated from the following equation:

$$k = -\frac{V_{slag}}{A_{slag-metal}} \frac{d\ln[wt.\%O]_{slag}}{dt} \tag{16}$$

The rate constant is plotted versus concentration for experiments at 1400 and 1600°C in Figure 11. The results show that the rate constant drops at low concentrations. Interpreted using Equation (15), Figure 11 shows that the mass transfer coefficient decreases at low concentrations of iron oxide in the slag.

In Figure 12 are data from experiments in which the slag initially contained 16 wt% total iron. It can be seen that the rate constant is not higher in these experiments than it was in

experiments 6 and 16. Comparison of the rate constant for the three sets of experiments at $[wt.\%O]_{slag} \cong 1.7$ shows that the rate constant is lowest for the experiments in which the slag initially contained 16 wt% total iron; at this level of $[wt.\%O]_{slag}$ the slags in experiments 1-7, 10, and 16 contained ferric iron. Slag sampling and analysis from experiments in which the slag initially contained 5 wt% total iron suggest that the ferric iron is consumed during the early part of the experiments. It is therefore likely that in experiments 9 and 17-19, when $[wt.\%O]_{slag} \cong 1.7$, only ferrous iron remained in the slag.

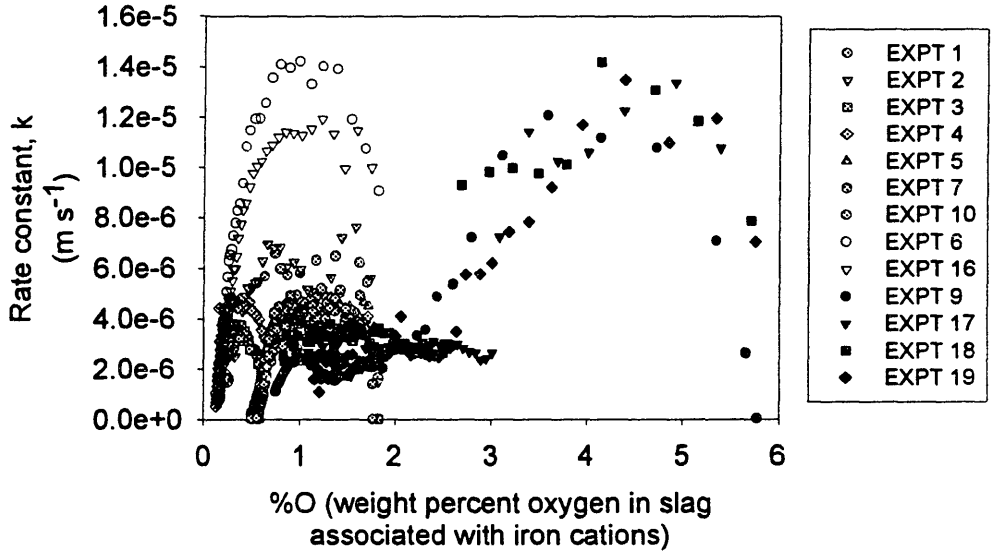

Figure 12. Plot of the rate constant *vs.* concentration for 5 or 16 wt% Fe slag

4.3 Short-circuit experiment #1

The purpose of this experiment was to test the hypothesis that the reaction rate is increased by short-circuiting the slag layer with a metallic conductor. An iron (low-carbon steel) "flag" was positioned so that it was above the molten Fe-C and base slag initially (Figure 13). The steel flag was made by welding a 1.27 cm (0.5 in.) diameter steel rod onto a piece of steel 9.5 cm (3.75 in.) wide, 3.8 cm (1.5 in.) high, and 0.48 cm (0.1875 in.) thick.

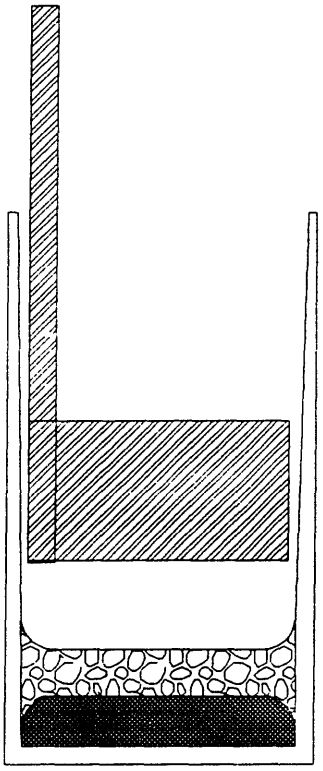

Figure 13. Iron flag in "up" position

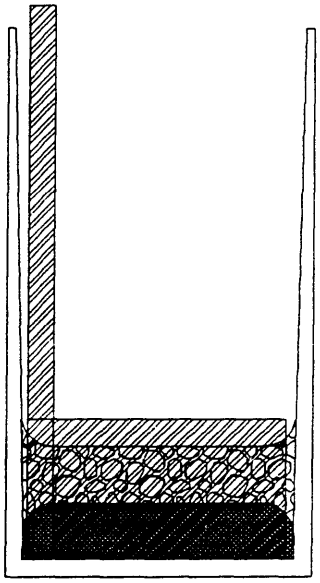

Figure 14. Iron flag in "down" position

With molten Fe-C and base slag in an alumina crucible, 2.78 g of pure Fe_2O_3 was dropped into the crucible. (The Fe_2O_3 powder was pressed into pellets.) The rate of CO evolution rose soon thereafter (see first "rise" in Figure 15). After the reaction subsided, the iron flag was lowered so that it penetrated the slag layer and made contact with the metal layer (Figure 14).

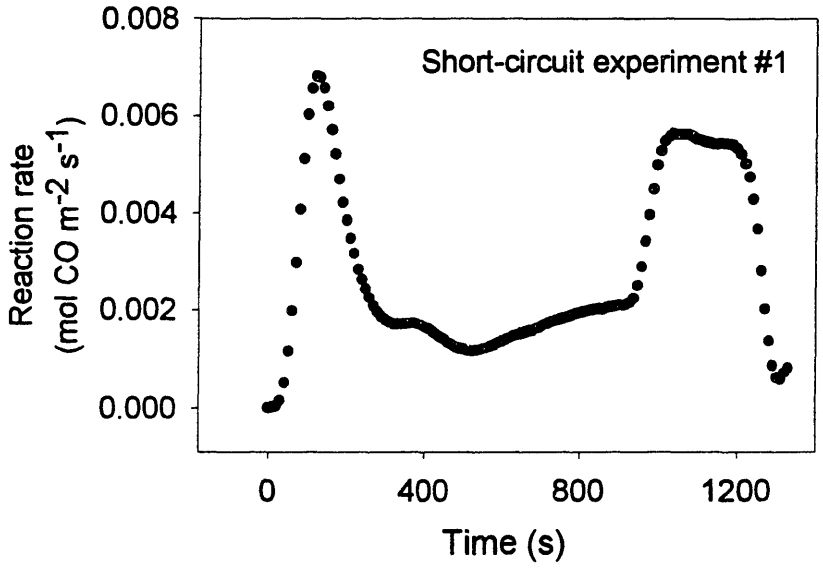

Figure 15. The reaction rate increased after lowering the iron plate

Approximately two minutes after the flag was lowered, the concentration of CO in the outlet gas stream (as measured by the CO analyzer) increased. Since the inlet flow rate of argon was constant during the experiment (approximately 0.53 SLPM(N_2), or 0.73

L(STP) argon min^{-1}, in this experiment), the increase in the CO concentration in the outlet gas stream translates into an increase in the reaction rate (see second "rise" in Figure 15). The reaction rate was calculated using Equation (6).

The delay between the lowering of the flag and the rise in the measured reaction rate is due to the length of gas line between the inner furnace chamber and the CO analyzer (Figure 3). (The iron flag was lowered at approximately 800 s. Refer to Figure 15.) The iron flag was held loosely in the furnace top, so it could slide down as the iron flag melted into the Fe-C bath. Approximately seven minutes after the flag was lowered, it had melted in enough so that the rod passed through the hole in the furnace top; the hole was then plugged with a short steel rod.

4.4 Short-circuit experiment #2

The purpose of this experiment was to test the following hypotheses: (1) the reaction rate is increased by short-circuiting the slag layer; and (2) the degree to which the reaction rate is increased by short-circuiting is proportional to the area of contact between the slag and the short-circuit material. An iron flag of the same dimensions as before was positioned above the slag layer. With molten Fe-C and base slag in an alumina crucible, 3.07 g of Fe_2O_3 was added in the form of pellets. The reaction rate rose quickly (see first

rise in Figure 16). At approximately 1100 s, the iron flag was lowered, and the reaction rate increased (Figure 16).

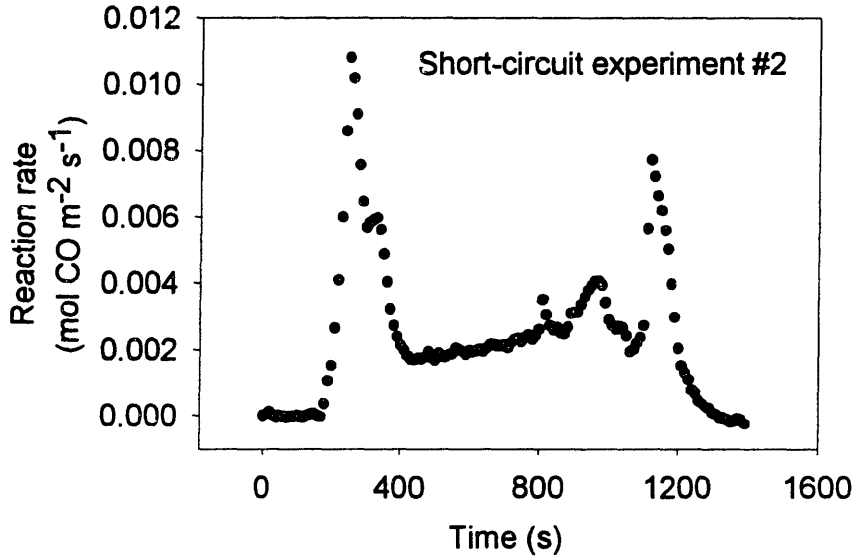

Figure 16. The results of short-circuit experiment #1 were confirmed

The time lag between lowering the flag and observing the increase in the CO concentration was much shorter in this experiment for two reasons. First, the flow rate of argon through the inner chamber was four times higher than in short-circuit experiment #1 (2.9 L(STP) min^{-1} versus 0.73 L(STP) min^{-1}). Second, and more importantly, the suction pump in the CO analyzer was working properly during this experiment, whereas it had not been working during short-circuit experiment #1.

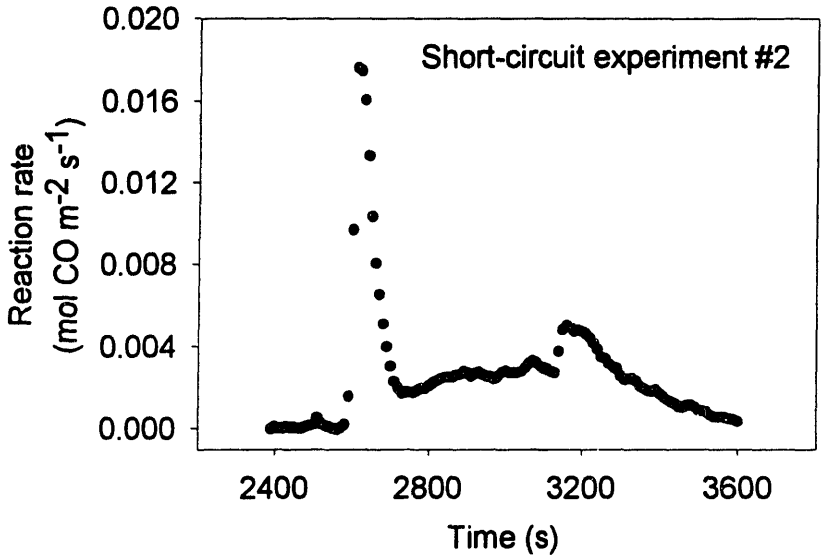

Figure 17. The increase in reaction rate was smaller when a rod was used

During this experiment, the rod attached to the iron flag was held tightly in the furnace top, so that it could not slide down. The flag and the lower portion of the rod melted into the Fe-C bath over several minutes after the flag was lowered. After the reaction rate dropped again, approximately fifteen minutes were allowed to pass, and then 3.15 g of Fe_2O_3 was added to the slag layer. This resulted in another rise in the reaction rate (Figure 17). At approximately 3100 seconds (elapsed time), the remaining iron rod was lowered so that it penetrated the slag layer and made contact with the metal bath. The reaction rate increased, and the increase was smaller than when the whole flag penetrated through the slag layer. (The carbon concentration was no doubt reduced because the flag melted into the liquid iron bath, but the concentration was still high enough so that the

reaction rate was most likely limited by mass transport of iron oxide in the slag phase. See Appendix E. Carbon concentration during short circuit experiments #1 and #2.)

4.5 Short-circuit experiment #3

The purpose of this experiment was to measure the "short-circuit current." This is the current that flows from the metal bath through the short-circuit material. In the first two short-circuit experiments, the short-circuit was formed by the iron flag or rod—the short-circuit was "internal." Therefore, in short-circuit experiments #1 and #2, the short-circuit current could not be measured.

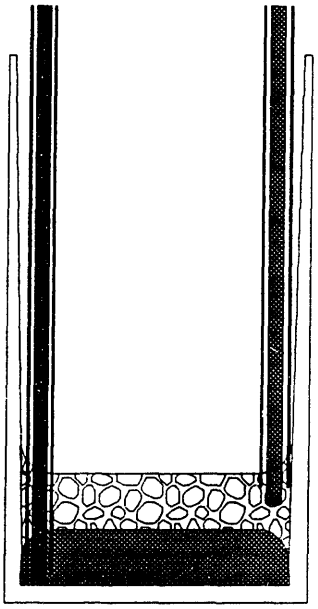

Figure 18. Apparatus for external short-circuit

In this experiment, the short-circuit was "external," and the short-circuit current could be measured. A graphite rod with a diameter of 0.64 cm (0.25 in.) was lowered so that it made contact with the Fe-C bath; an alumina tube prevented the slag from contacting the graphite rod (Figure 18). A molybdenum rod with a diameter of 0.64 cm (0.25 in.) was lowered so that it made contact with the slag layer; an alumina tube prevented the gas phase from contacting the molybdenum rod.

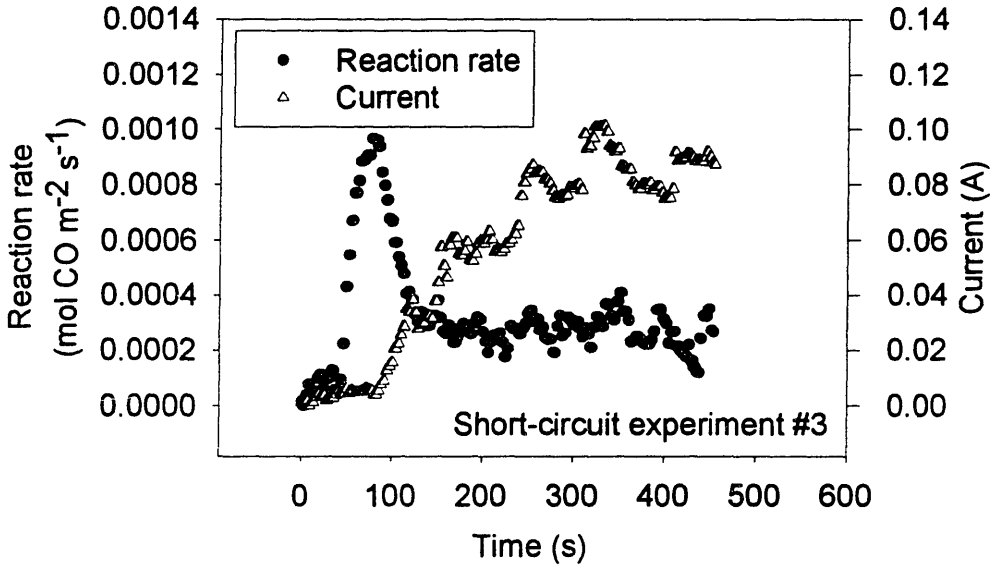

Figure 19. A short-circuit current was observed after adding iron oxide

Once the base slag and Fe-C metal were melted, 3.40 g of 'FeO' was added. (The 'FeO' was in the form of approximately 5-mm pieces, obtained by crushing commercial 'FeO' pellets.) The reaction rate rose quickly (Figure 19). Later, the current rose; electrons

were flowing from the graphite rod through the external circuit to the molybdenum rod. When the reaction rate (and short-circuit current) had subsided to zero, 7.04 g 'FeO' was added to the slag layer. The reaction rate rose quickly (Figure 20). A bit later, the short-circuit current rose.

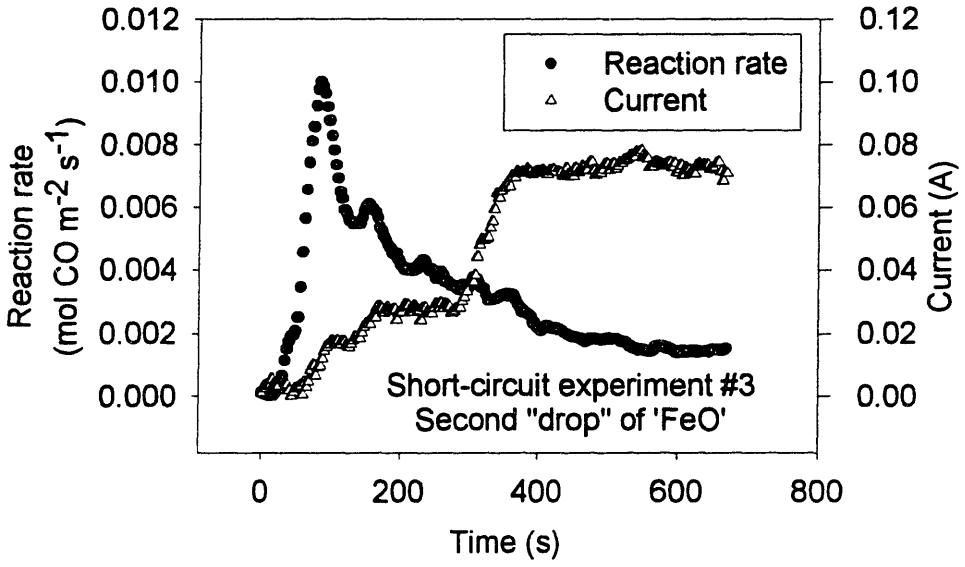

Figure 20. A short-circuit current was observed again

The data in Figure 19 and Figure 20 can be explained by the sequence of events now described. When the FeO pellets fell on the surface of the base slag, they floated; this was observed through a sight glass. Through convection of the slag, pure FeO, or slag very high in FeO, was brought in contact with the slag-metal interface. At this point, the reaction rate rose rapidly. The CO gas evolved as a result of this initial burst of reaction

stirred the slag phase, and distributed the remaining unreacted FeO evenly throughout the slag phase. At this time, slag containing iron oxide contacted the molybdenum rod, and a short-circuit current arose. Some of the electrons produced in the anodic reaction in Equation (2) at the slag-metal interface flowed through the external circuit to the interface between the molybdenum rod and the slag phase. There they were consumed by the cathodic reactions in Equations (3) and (4).

4.6 Decarburization experiment #1

The purpose of this experiment was to confirm that the steady-state rate of decarburization by CO_2 through a slag containing iron oxide is proportional to the iron oxide concentration in the slag phase. With argon gas flowing through the inner chamber, 3.43 g of FeO was added to the molten base slag. (The FeO, obtained from a chemical supply company, was crushed so that all pieces were less than 2 mm.) The CO concentration temporarily rose after this "drop," as it did during the short-circuit experiments when a drop of iron oxide was made. A mixture of Ar-6 vol% CO_2 was passed through the inner furnace chamber, and the CO concentration rose to a steady value of approximately 0.4% CO.

Then the CO_2 flow was shut off and only argon was passed through the inner furnace chamber. The CO concentration reading fell to less than 0.1 %CO. An additional 4.33 g of the same FeO was added to the molten base slag. A gas mixture of Ar-6% CO_2 was passed, and the CO concentration rose to approximately 0.7% CO.

A flow of pure argon was resumed, and the CO concentration fell to about 0.35% CO. A mass of 3.21 g of 'FeO' was then added to the molten slag layer. (This 'FeO' was crushed to approximately 5-mm pieces, obtained from commercial 'FeO' pellets.) The reaction rate temporarily rose, and then fell. The flow of Ar-6% CO_2 was resumed, and the CO concentration rose to approximately 1% CO.

The steady-state decarburization rate as a function of FeO concentration in the slag can be estimated using Equation (6) (see Table VI). Calculations show that there was plenty of CO_2 available for oxidation of the slag. (See Appendix F. Flux of CO in decarburization experiment #1.)

Table VI . The rate of decarburization increased with FeO concentration

wt% FeO	Steady-state decarburization rate (mol CO m^{-2} s^{-1})
1.1	$1.3 \cdot 10^{-3}$
2.6	$2.3 \cdot 10^{-3}$
3.6	$3.1 \cdot 10^{-3}$

4.7 Decarburization experiment #2

The purpose of this experiment was to test the hypothesis that the steady-state rate of decarburization by CO_2 through a slag phase containing iron oxide could be increased by applying a voltage between the cathode (in the slag) and the anode (in the metal bath). In the first part of this experiment, the apparatus in Figure 18 was used; an alumina tube prevented the molybdenum rod from contacting the gas phase. Iron oxide was added to the slag layer, so that the slag contained approximately 3.5 wt% FeO. A mixture of Ar-6 vol% CO_2 was passed through the inner furnace chamber. The slag was electrolyzed; the current observed as a function of applied voltage for this case of a "shielded" electrode is shown in Figure 21.

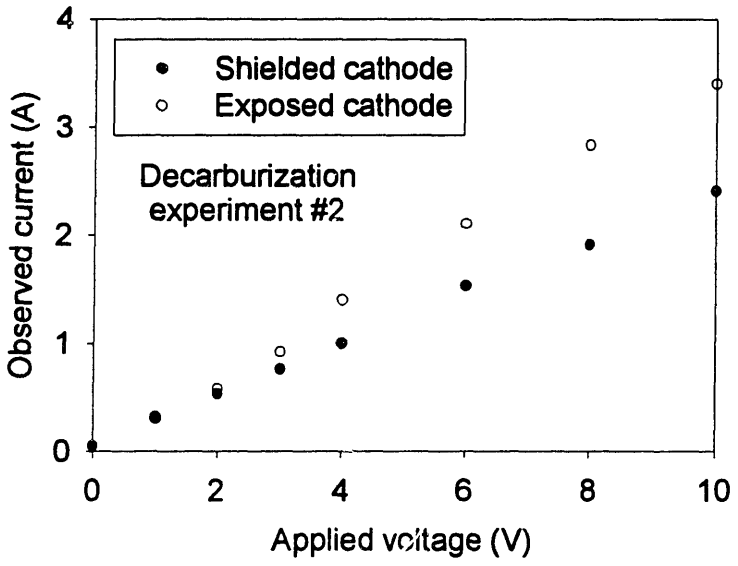

Figure 21. Plot of current *vs.* voltage for decarburization experiment #2

The reaction rate in terms of CO responded to the passage of current. When the applied voltage was 10 V, the CO concentration was approximately 0.75, and when the applied voltage was reduced to 0 V, the CO concentration fell to approximately 0.60. If the electrolysis was Faradaic, then the change in reaction rate would be proportional to the current,

$$\Delta r = \frac{1}{zFA} I \tag{17}$$

where z is the number of equivalents per mole of CO, F is the Faraday constant, and A is the slag-metal interfacial area. The observed change in current (in passing from a voltage

of 0 V to 10 V) was approximately 2.4 A (Figure 21). If the anodic reaction is that given in Equation (2), and the cathodic reaction is that given in Equation (3) or Equation (4), then there are two equivalents per mole of CO. Using the slag-metal interfacial area in Table IV, one calculates that the expected change in the reaction rate is $2.4 \cdot 10^{-3}$ mol CO m^{-2} s^{-1}. Using Equation (6), and the fact that the total gas flow rate was 1.6 SLPM(N_2), one calculates that the observed change in the reaction rate was $4.9 \cdot 10^{-4}$ mol CO m^{-2} s^{-1}, which implies that the current efficiency was 20%.

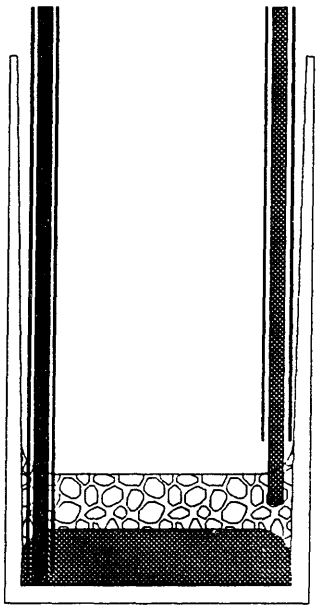

Figure 22. Molybdenum cathode is exposed to CO_2 in the gas phase

In the second part of the experiment the alumina tube around the molybdenum rod was raised a bit, so that the gas phase could contact the molybdenum rod at the interface between the rod and the slag phase (Figure 22). The slag was electrolyzed again, and the

observed current in this case of an "exposed" cathode was higher than when the molybdenum rod was shielded from the gas phase (Figure 21).

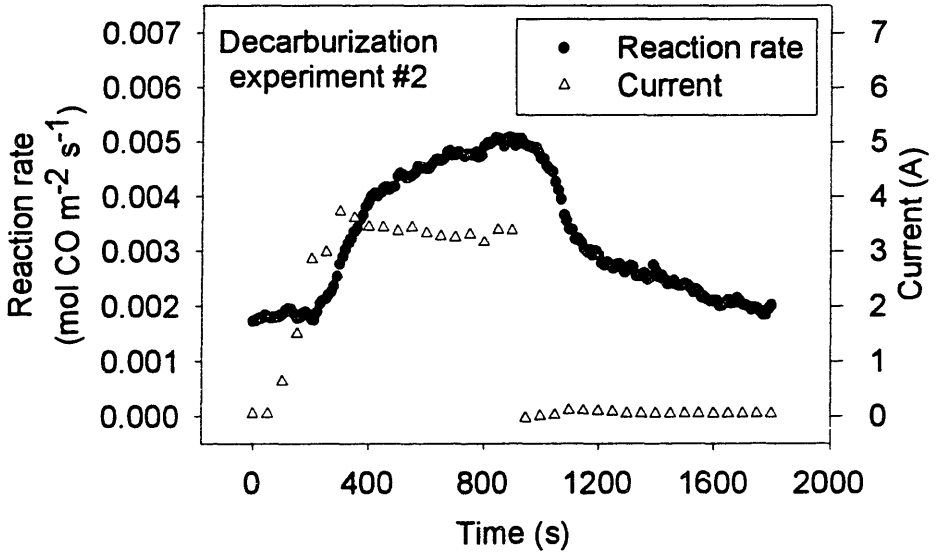

Figure 23. The decarburization rate increased when a molybdenum cathode was used

The reaction rate in terms of CO increased when voltage was applied across the slag layer (Figure 23). The current increased 3.4 A (Figure 21), and the CO concentration increased 1% CO. Suppose that the electrolysis was Faradaic, the anodic reaction is that given in Equation (2), and the cathodic reaction is

$$(CO_2)+2e^- \rightarrow (CO)+\left[O^{2-}\right]_{slag}. \qquad (18)$$

Under these conditions, there is one equivalent per mole of CO. The expected increase in reaction rate is $6.7 \cdot 10^{-3}$ mol CO m^{-2} s^{-1}. The observed increase in reaction rate was approximately $3.0 \cdot 10^{-3}$ mol CO m^{-2} s^{-1}, which implies a current efficiency of 45%. (If the anodic reaction is that given in Equation (2) and the cathodic reaction is given in Equation (3) or Equation (4), then there are two equivalents per mole of CO, and the current efficiency is 90%.)

4.8 Decarburization experiment #3

The purpose of this experiment was to test the hypothesis that the current efficiency was limited in the previous decarburization electrolysis experiments by the area of the slag-molybdenum rod interface; the investigators thought that the current efficiency might be increased if the current density could be decreased. In this experiment, a DC electric arc was generated between a graphite rod held above the slag layer, and the surface of the slag layer. The electric arc served as the cathode. The anode was a graphite rod dipped into the Fe-C bath, and this rod was protected from contacting the slag by an alumina tube.

Iron oxide in the form of commercial 'FeO' pellets was dropped into the molten base slag, so that the iron oxide concentration was approximately 3.1 wt% FeO. A gas mixture Ar-6 vol% CO_2 was passed through the inner furnace chamber. The CO concentration achieved a steady reading of approximately 1.1 % CO, and the total gas

flow rate was 1.76 SLPM(N_2). Using Equation (6), one calculates that the steady-state rate of decarburization was $4.0 \cdot 10^{-3}$ mol CO m^{-2} s^{-1}, in reasonable agreement with decarburization experiment #1 (Table VI).

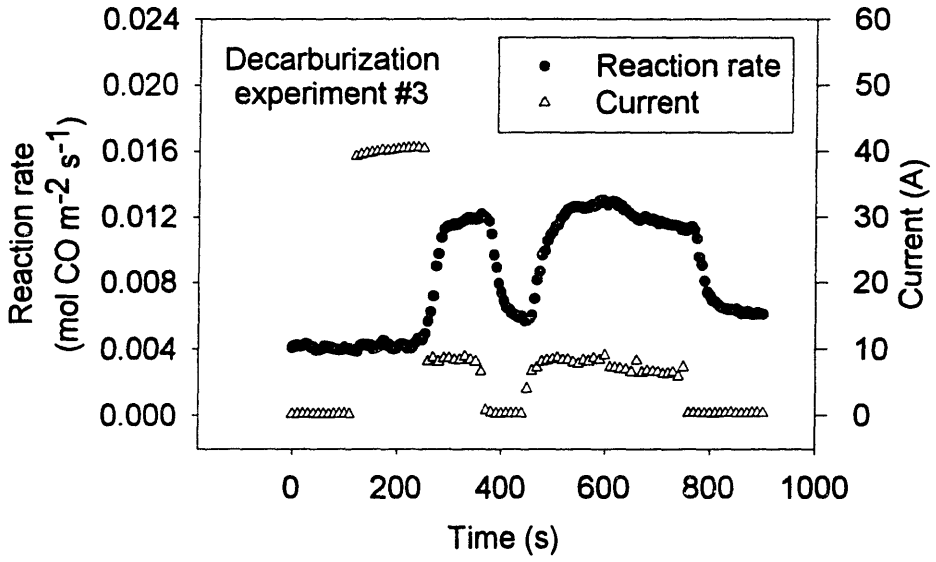

Figure 24. The decarburization rate increased when an electric arc cathode was used

Both graphite rods were dipped in the metal phase, and a current of 40 A was passed with 13 V. One graphite rod was then raised 4 cm off the bottom of the crucible. (The graphite rod was raised with a pulley-and-string system, so that the current could keep flowing while the rod was raised.) An electric arc was formed, and a current of 8 A was passed at 53 V. The decarburization rate increased when the anode was raised out of the metal bath (Figure 24), even through the current decreased. (The arc "went out"

temporarily at about 350 seconds, and was then reestablished; the current dropped to zero and the reaction rate fell when the arc went out.)

If the electrolysis was Faradaic, the anodic reaction is given in Equation (2) and the cathodic reaction is given in Equation (18), then there is one equivalent per mole of CO. Given the current of 8 A, the expected reaction rate is $1.6 \cdot 10^{-2}$ mol CO m^{-2} s^{-1}. The observed increase in reaction rate was approximately $8.0 \cdot 10^{-3}$ mol CO m^{-2} s^{-1}, which implies a current efficiency of 50%. (If the anodic reaction is given in Equation (2) and the cathodic reaction is given in either Equation (3) or Equation (4), then there are two equivalents per mole of CO, and the current efficiency is 100%.)

4.9 Reduction experiment #1

The purpose of this experiment was to test the hypothesis that the rate of reduction of iron oxide from slag could be increased by applying a voltage between the cathode (in the slag) and the anode (in the metal bath). The apparatus used in this experiment is shown in Figure 18. Iron oxide was added to the slag, so that the FeO concentration was approximately 3.5 wt%. Argon gas was passed through the inner furnace chamber. The reaction rate increased after the addition, and after some time dropped to a very low level.

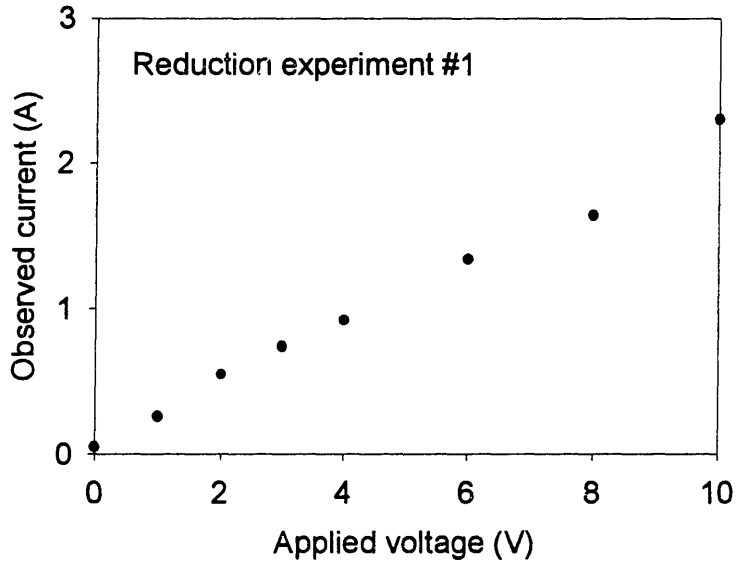

Figure 25. Plot of current *vs.* voltage for reduction experiment #1

The voltage was increased in steps and the current was recorded at each step (Figure 25). The rate of CO evolution increased as the current increased (Figure 26). Suppose that the electrolysis is Faradaic, the anodic reaction is given in Equation (2) and the cathodic reaction is given in either Equation (3) or Equation (4). Then there are two equivalents per mole of CO. For a current rise of 2.25 A, the reaction rate should increase by $2.2 \cdot 10^{-3}$ mol CO m^{-2} s^{-1}. The observed increase was approximately $8 \cdot 10^{-4}$ mol CO m^{-2} s^{-1}, which implies a current efficiency of 36%.

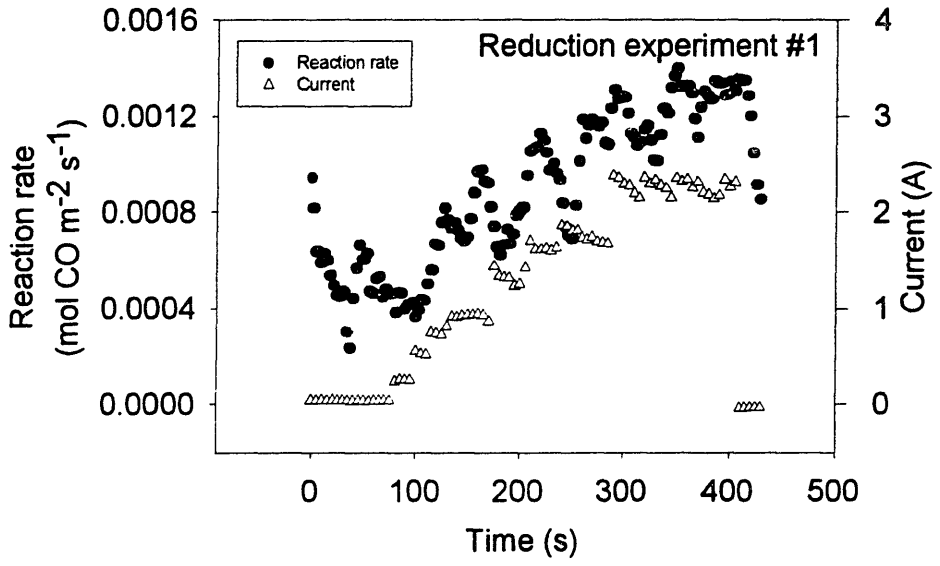

Figure 26. The reduction rate increased when a molybdenum cathode was used

4.10 Reduction experiment #2

The purpose of this experiment was to test the hypothesis that the current efficiency was limited in reduction experiment #1 by the area of the slag-molybdenum rod interface. In this experiment, a DC electric arc was generated between a graphite rod held above the slag layer, and the surface of the slag layer; the electric arc served as the cathode. The anode was a graphite rod dipped into the Fe-C bath; the anode was protected from contacting the slag by an alumina tube.

Argon was passed through the inner chamber during the experiment. One graphite rod was lowered to the bottom of the crucible; it was protected by an alumina tube, except over a length of 0.5 cm at the bottom. A second graphite rod was positioned so that its bottom end was 4.6 cm from the bottom of the crucible; its lower end was above the molten metal layer. The 100A-100VDC EMI power supply was turned on and set for 10 A (constant current mode); the electrodes were under "live" power at this point, and the voltage across them was 100VDC.

A mass of 167 g of crushed, pre-fused, iron oxide-containing slag was dropped into an alumina crucible holding molten Fe-C. The slag had 5.00 wt% total iron, and 2.22 wt% ferrous iron, as determined by wet chemical analysis. (The slag had been made earlier by adding iron oxide to molten base slag.) The slag melted and began to react with the Fe-C bath; the rate of CO evolution rose to approximately 0.015 mol CO m^{-2} s^{-1} (Figure 27).

The slag began to foam, so the slag level rose in the crucible. About six minutes after the slag was added to the crucible, the current rose from zero to 10 A, and when this happened, the reaction rate rose to approximately 0.025 mol CO m^{-2} s^{-1} (Figure 27).

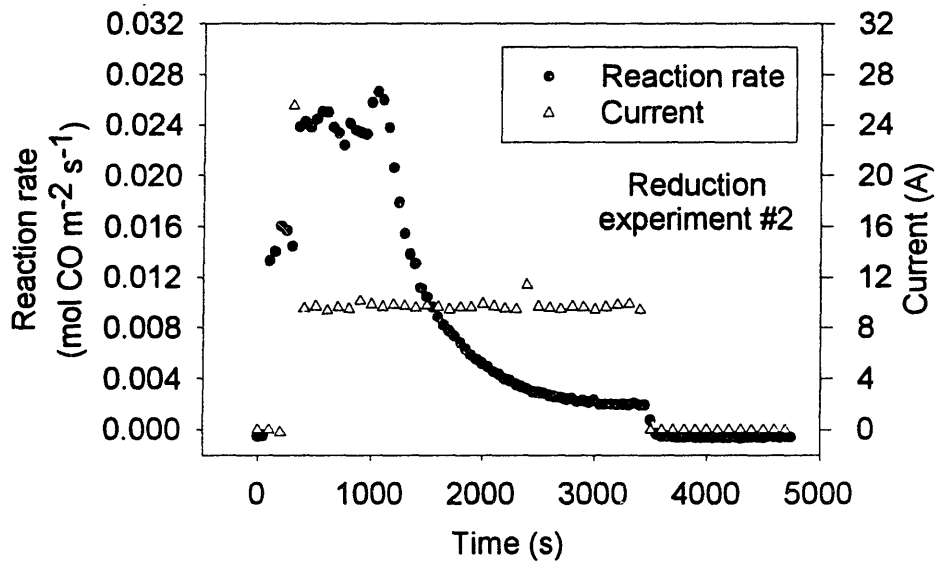

Figure 27. The reduction rate increased when an electric arc cathode was used

If the electrolysis is Faradaic, the anodic reaction is given in Equation (2) and the cathodic reaction is given in either Equation (3) or Equation (4), then there are 2 equivalents per mol CO. For a current of 10 A, the expected increase in reaction rate is $9.8 \cdot 10^{-3}$ mol CO m^{-2} s^{-1}. The observed increase was approximately $1.0 \cdot 10^{-2}$ mol CO m^{-2} s^{-1}, so the current efficiency was nearly 100% when the current first began to flow.

At 1000 s the reaction rate began to fall. That is, the rate of CO evolution began to fall. The applied voltage decreased during the experiment (Figure 28), even though the current remained constant (Figure 27). Therefore, it is likely that the drop in the rate of CO evolution was due to electronic short-circuiting of the slag layer. (Metal is formed at the cathode. Also, metal is entrained in the slag layer by the vigorous stirring accompanying this relatively high reaction rate.)

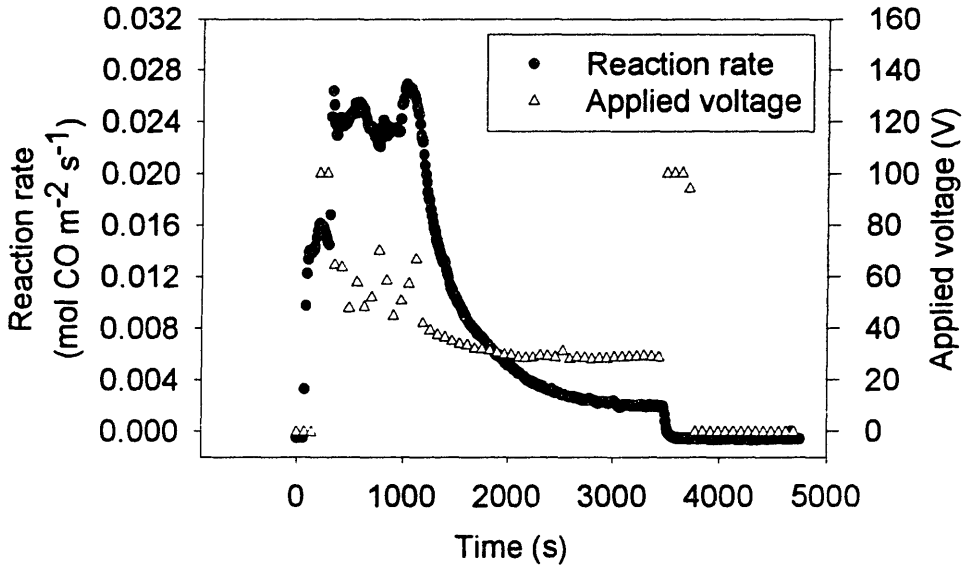

Figure 28. The voltage required to maintain constant current decreased over time

At the relatively high reaction rate obtained in this experiment, the concentration of iron oxide falls significantly during the experiment. The data in Figure 29 show that the

reaction rate in terms of CO began to fall when $[wt\%\ O]_{slag}$ was approximately 0.5. If all the iron in the slag was ferrous at this point, then this corresponds to 2.2 wt% FeO.

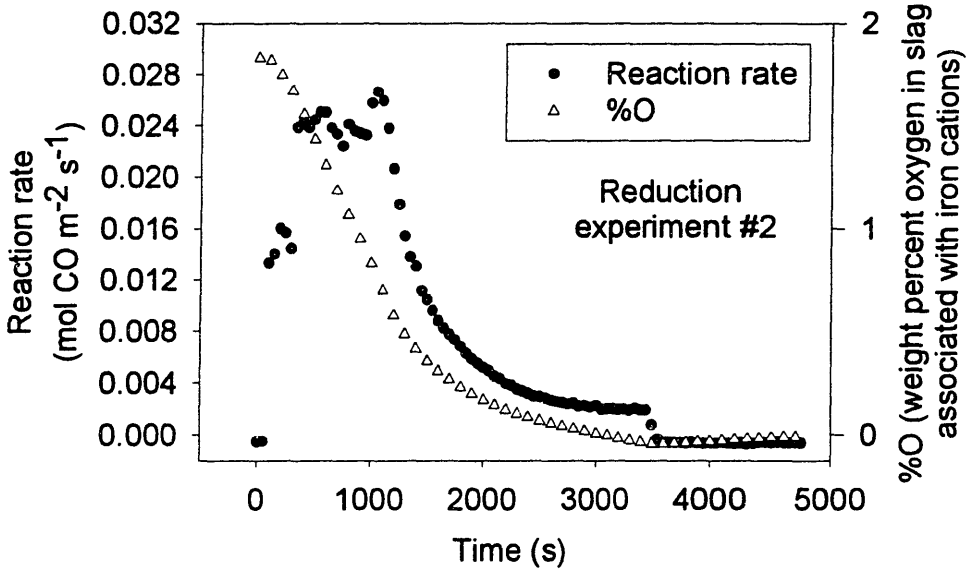

Figure 29. The reaction rate decreased as the value %O reached 0.5

4.11 Reduction experiment #3

In reduction experiment #2, the current efficiency was 100% for a significant period of time (approximately 20 minutes). It was expected that if the current density were higher, then electronic short-circuiting due to metal formation at the cathode would occur more

quickly during an experiment. For this reason, it was expected that as the current density increased, the period of 100% current efficiency would become shorter.

The plan for this experiment was to use an electric arc as the cathode, as in reduction experiment #2, but to use a current of 20 A (i.e. twice that used in reduction experiment #2). If the area of arc-slag contact was the same, then the current density would double. In other respects, this experiment was conducted in the same manner as reduction experiment #2. The amount of slag added in this experiment was 177 g.

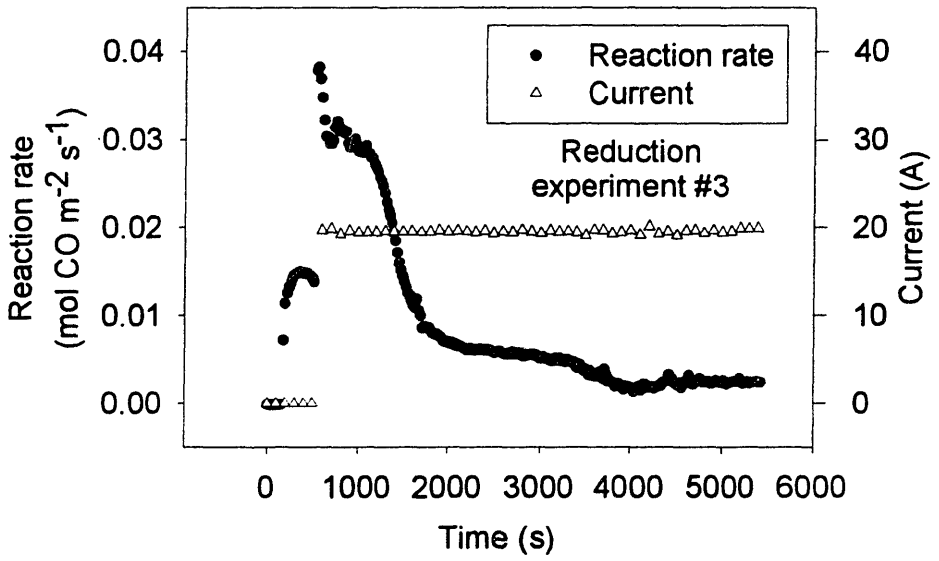

Figure 30. The reaction rate increased more when a higher current was used

The 100A-100VDC EMI power supply was in constant-current mode set for 20 A. About nine minutes after the slag was added to the crucible, the observed current rose to 20 A, and the reaction rate in terms of CO increased (Figure 30). For a current of 20 A, the expected increase in reaction rate is $2.0 \cdot 10^{-2}$ mol CO m^{-2} s^{-1}. The reaction rate briefly rose to $2.0 \cdot 10^{-2}$ mol CO m^{-2} s^{-1}, and then fell quickly to approximately $1.5 \cdot 10^{-2}$ mol CO m^{-2} s^{-1}. In other words, the current efficiency was briefly 100%, and then fell to approximately 75%.

Chapter 5. Discussion

5.1 New expression for the mass transfer coefficient

The usual "power-law" rate expression for an n^{th} order chemical reaction has the following form:

$$r\left[\frac{\text{mol}}{\text{m}^2\,\text{s}}\right] = kc^n \tag{19}$$

where r is the overall reaction rate, k is the rate constant, c is concentration, and n is the order of reaction. Most investigators who have studied the rate of reduction of iron oxide from slag by carbon have concluded that a first-order model fits their data.

$$r = kc \tag{20}$$

where c is the concentration of iron oxide in the slag. For a first-order model, the rate constant has units of m s^{-1}, since the concentration has units of mol m^{-3}.

In nearly all previous studies of the reduction of iron oxide from slag, ferrous oxide (FeO) has been used to make the slags, so that the slag contains mostly ferrous iron (Fe^{2+}), and very little ferric iron (Fe^{3+}). The concentration of iron oxide in the slag is usually expressed as wt% FeO.

$$r = k\left[wt.\%FeO\right]_{slag} \tag{21}$$

(The rate constant must have appropriate units.) In these experiments, where only ferrous cations are present in the slag, there is a one-to-one correspondence between the flux of the following species to the slag-metal interface:

- ferrous cations (in the slag phase)
- oxygen (in the slag phase)
- carbon (in the metal phase)

This follows from the stoichiometry of the reaction in Equation (1). The "reaction rate in terms of ferrous iron," the "reaction rate in terms of carbon," the "reaction rate in terms of CO," are all the same (on a molar basis).

$$r_{Fe^{2+}} = r_C = r_{CO} \tag{22}$$

Under these conditions one could monitor the reaction rate by any of the following methods:

- slag sampling and analysis for ferrous iron
- metal sampling and analysis for carbon concentration
- measuring the rate of CO evolution.

Since there is only ferrous iron in the slag phase, the "reaction rate in terms of total iron (in the slag phase)" is equal to the reaction rate in terms of ferrous iron, and one could monitor the reaction rate by slag sampling and analysis for total iron. If there is no CO_2 evolution, then the "reaction rate in terms of oxygen" is equal to the reaction rate in terms of CO. In this study, the reaction rate in terms of oxygen, r_O, was observed by measuring the rate of CO evolution.

Plots of the rate constant, k, versus concentration show that k is, in fact, not constant, but decreases as the concentration of iron oxide decreases (Figure 11 and Figure 12). This observation supports the hypothesis that the reaction rate is limited by the rate of mass transport of ferrous cations in the slag phase when the slag contains very little ferric oxide. If this hypothesis is true, then the reaction rate in terms of oxygen is equal to the flux of ferrous cations to the slag-metal interface.

$$r_O = J_{Fe^{2+}} \tag{23}$$

The flux of ferrous cations can be written in terms of the concentrations of ferrous cations in the bulk of the slag and at the slag-metal interface.

$$J_{Fe^{2+}} = k_D\left(c_{Fe^{2+}}^{bulk} - c_{Fe^{2+}}^{interface}\right) \tag{24}$$

A gradient in the concentration of ferrous cations will exist in the slag phase adjacent to the slag-metal interface (Figure 31). The constant k_D is called the mass transfer coefficient. If the reaction rate is limited by mass transport of ferrous cations, then the concentration of ferrous cations at the slag-metal interface will be equal to the equilibrium concentration.

For the reduction of ferrous oxide from slag by carbon in iron, calculations show that the equilibrium concentration of ferrous oxide in the slag is very nearly zero. (See Appendix B. Concentration of FeO in slag in equilibrium with liquid.) One can simplify Equation (24) by setting the interfacial concentration to zero.

$$J_{Fe^{2+}} \cong k_D c_{Fe^{2+}}^{bulk} \tag{25}$$

Substitution of Equation (25) into Equation (23) gives the relation

$$r_O = k_D C_{Fe^{2+}}^{bulk} \tag{26}$$

which is of the same form as Equations (20) and (21)—a reaction rate that is first order in the concentration of ferrous oxide or ferrous cations. The fact that so many investigators have observed that this type of equation fits their data is evidence that the overall reaction rate is limited by mass transfer of ferrous cations in the slag phase when the slag contains very little ferric oxide.

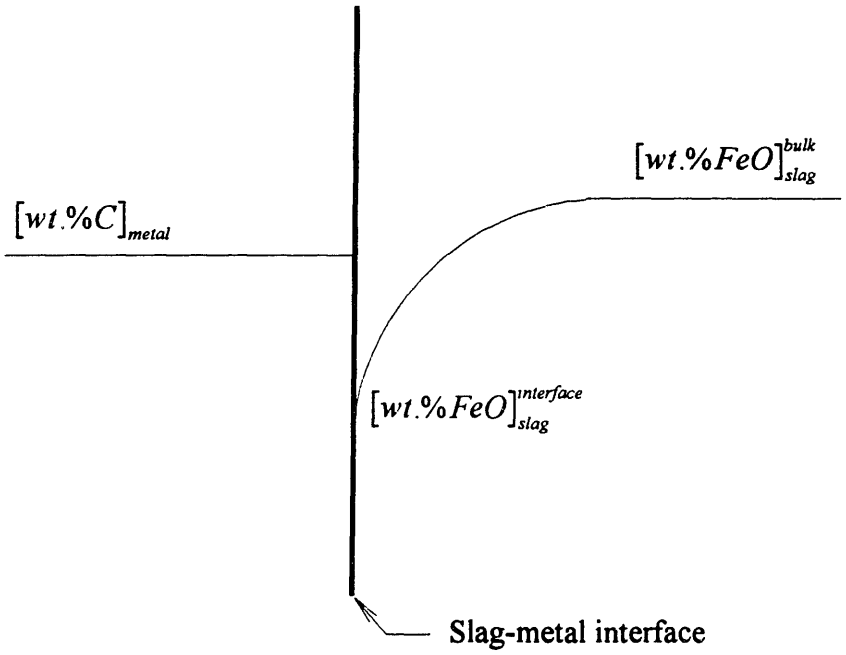

Figure 31. Slag near the slag-metal interface is depleted in iron oxide

Some studies have shown a reaction order higher than one (Table I), or a reaction order that changes with concentration. (In these studies only ferrous cations were present in the

slag since FeO was used to make the slags.) To understand this observation, one needs to examine the dependence of the mass transfer coefficient on the reaction rate or concentration. If fluid flow conditions in the slag remained constant during the course of an experiment, then one would expect that the mass transfer coefficient would remain constant, and that the reaction would be first-order in FeO or Fe^{2+} concentration (Equation (26)).

However, there is vigorous stirring of the slag when the reaction rate is high, and little stirring when the reaction rate is low, so the fluid flow conditions in the slag change during the course of the reaction. One therefore expects that the mass transfer coefficient will decrease as the reaction rate decreases, or, equivalently, that the mass transfer coefficient will decrease as the concentration of FeO decreases. The data in Figure 11 and Figure 12 show that k_D decreases at low concentration. In other words, the mass transfer coefficient depends on the concentration of ferrous cations in the slag at low concentrations.

A power-law relationship can be used to describe the dependence of the mass transfer coefficient, k_D, on the concentration of ferrous cations in the slag, c:

$$k_D = B' c^p \tag{27}$$

where B' and p are a positive constants. (See Appendix H. Analysis of results using dimensionless numbers.) Substitution of Equation (27) into Equation (26) yields

$$r_O = k_D c = B' c^{1+p} \tag{28}$$

If the constant p is greater than zero, the reaction rate is greater than first-order. The dependence of the mass transfer coefficient on the reaction rate, or the concentration, is therefore an explanation for the observation of reaction orders higher than one.

Wagner[13] used this approach to explain the second-order kinetics observed in the early study by Philbrook and Kirkbride[5]. Most subsequent studies, done at higher concentrations of FeO in the slag, have shown that the kinetics are first-order. However, Philbrook and Kirkbride used low concentrations of FeO (Table II), so they were in the regime where the mass transfer coefficient depends on the concentration. The particular value of the concentration at which the mass transfer coefficient begins to decrease must depend on, among other things, the temperature and the base slag composition.

Wagner[13] proposed that the diffusion boundary layer thickness depends on the reaction rate according to the following equation:

$$\delta = \frac{B}{r^{\beta}} \tag{29}$$

where B and β are positive constants. (This equation gives the thickness, δ, of the diffusion boundary layer for iron cations in the slag layer adjacent to the slag-metal interface.) His idea in proposing Equation (29) was that the boundary layer thickness must decrease as the reaction rate increases, since the increasing gas evolution would cause more vigorous convection in the slag phase.

Two models of the mass transfer coefficient are typically used to give the mass transfer coefficient a "physical" meaning. In the first, the mass transfer coefficient is written in terms of the diffusivity, D, and the "diffusion boundary layer thickness," δ.

$$k_D = \frac{D}{\delta} \tag{30}$$

In the second, the mass transfer coefficient is written in terms of D and the "contact time," θ.

$$k_D = \sqrt{\frac{4D}{\pi\theta}} \tag{31}$$

According to Equation (30), if the diffusion boundary layer thickness increases, then the mass transfer coefficient decreases. Similarly, Equation (31) implies that if the contact time increases, then the mass transfer coefficient decreases.

Equation (29) implies that the boundary layer thickness tends toward zero for very high reaction rates. The following modification of Equation (29) is proposed:

$$\delta = \frac{B}{r^{\beta}} + \delta_o \tag{32}$$

where B and β are constants, and $0 \le \beta < 1$. Equation (32) implies that the effective boundary layer thickness approaches some minimum value as the reaction rate grows large. If the constant B is small, then the first term in the sum only becomes significant when the reaction rate falls to a fairly low value. If Equations (32) and (26) are substituted into Equation (30), one can obtain the following expression for the mass transfer coefficient as a function of concentration:

$$k_D = \frac{D}{\frac{B}{k_D^{\beta} c^{\beta}} + \delta_o} \tag{33}$$

At high concentrations, Equation (33) reduces to

$$k_D = \frac{D}{\delta_o} \tag{34}$$

whereas at low concentrations, it reduces to

$$k_D = \left(\frac{D}{B}\right)^{\frac{1}{1-\beta}} c^{\frac{\beta}{1-\beta}} \tag{35}$$

For $\beta = 1/3$, for example, the mass transfer coefficient is proportional to the concentration to the one-half power, $k_D \propto \sqrt{c}$. On the other hand, if $\beta = 1/2$, then $k_D \propto c$.

Figure 11 and Figure 12 show the relationship between the mass transfer coefficient and the concentration observed in the first part of this study. (See also Appendix H. Analysis of results using dimensionless numbers.) At low concentrations (in terms of $[wt\%\ O]_{slag}$), the results show that the mass transfer coefficient varies with concentration according to the proportionality $k_D \propto c^m$ where $m \cong 1$. Therefore, the reaction rate is first-order in the concentration of ferrous cations at high concentrations, and the order of reaction increases at low concentrations. In other words, the effect of concentration on the mass transfer coefficient becomes relatively more significant at low concentrations, a conclusion which at first might seem counter-intuitive. Note that Tarby and Philbrook[6],

who considered the effect of CO evolution on the fluid flow conditions in the slag, actually concluded the opposite; namely, that the reaction rate is second-order in iron oxide concentration at high concentrations, and is first-order at low concentrations.

A similar approach can be used, based on the contact-time model. The contact time is related to the reaction rate by the following equation:

$$\theta = \frac{C'}{r^{\chi}} + \theta_o \tag{36}$$

where C' and χ are constants, and $0 \le \chi < 2$. If Equations (36) and (26) are substituted into Equation (31), one can obtain the following expression for the mass transfer coefficient:

$$k_D = \frac{2D^{1/2}}{\pi^{1/2}\left(\frac{C'}{k_D^{\chi} c^{\chi}} + \theta_o\right)^{1/2}} \tag{37}$$

At high concentrations, Equation (3) reduces to

$$k_D = \sqrt{\frac{4D}{\pi\theta_o}} \tag{38}$$

At low concentrations, it reduces to

$$k_D = \left(\frac{4D}{\pi C'}\right)^{\frac{1}{2-\chi}} c^{\frac{\chi}{2-\chi}} \tag{39}$$

For $\chi = 2/3$ the mass transfer coefficient is proportional to the concentration to the one-half power, $k_D \propto \sqrt{c}$. For $\chi = 1$, $k_D \propto c$.

To summarize, a good model of the reaction rate in terms of oxygen for the period when only ferrous cations are present in the slag is given by the following expression:

$$r_O = k_D c_{Fe^{2+}} = \begin{cases} \dfrac{D}{\dfrac{B}{k_D^{\beta} c_{Fe^{2+}}^{\beta}} + \delta_o} c_{Fe^{2+}} \\ \dfrac{2D^{1/2}}{\pi^{1/2}\left(\dfrac{C'}{k_D^{\chi} c_{Fe^{2+}}^{\chi}} + \theta_o\right)^{1/2}} c_{Fe^{2+}} \end{cases} \tag{40}$$

Note that in the Results section, the reaction rate and mass transfer coefficient have been plotted versus the quantity $[wt.\%O]_{slag}$. When only ferrous cations are present in the slag phase, the $[wt.\%O]_{slag}$ and $c_{Fe^{2+}}$ are related by the following equation:

$$[wt.\%O]_{slag} = \frac{1.6}{\rho_{slag}\left[\dfrac{\text{kg}}{\text{m}^3}\right]} c_{Fe^{2+}}\left[\frac{\text{mol}}{\text{m}^3}\right] \tag{41}$$

If the density of the slag is constant and equal to 2500 kg m^{-3}, then one obtains:

$$[wt.\%O]_{slag} = 6.4 \cdot 10^{-4} \cdot c_{Fe^{2+}}\left[\frac{\text{mol}}{\text{m}^3}\right] \tag{42}$$

where $c_{Fe^{2+}}$ is the concentration of ferrous cations in the slag in units of mol m^{-3}. If a slag contains 5 wt% FeO and the density is 2500 kg m^{-3}, then $c_{Fe^{2+}} \cong 1700$ mol m^{-3} and $[wt.\%O]_{slag} \cong 1.1$.

5.2 New rate expression

Using Equation (40) to model the reaction rate is fine when the concentration of ferric cations is low. However, when the concentration of ferric cations is significant, this approach must be abandoned. When ferric cations are present in the slag, some electrons are consumed by the ferric-to-ferrous reduction reaction (Equation (3)), and the reaction rate in terms of total iron (in the slag phase) is lower than the reaction rate in terms of CO. That is, oxygen is removed from the slag at a faster rate on a molar basis than iron is reduced to metallic iron.

Slag analysis data show that ferric cations are reduced before ferrous cations, so that after some time has passed, nearly all the iron cations remaining in the slag are ferrous (Figure 8). (See Appendix D. The rate constants.) During the first period of reaction, then, ferric cations are reduced to ferrous cations. At the beginning of the second period, only ferrous cations remain in the slag, and during the second period, ferrous cations are reduced to metallic iron.

It is proposed that the reaction rate in terms of oxygen can be modeled by an expression of the following form in the general case when ferrous and ferric cations are both present.

$$r_O = k_1\left[wt.\%Fe^{3+}\right]_{slag} + k_2\left[wt.\%Fe^{2+}\right]_{slag} \tag{43}$$

where k_1 and k_2 are constants.

When significant quantities of both ferric and ferrous cations are present in the slag, the reaction rate is very high, which makes the mass transfer coefficient for ferric cations, $k_D^{Fe^{3+}}$, and the mass transfer coefficient for ferrous cations, $k_D^{Fe^{2+}}$, very high. These two mass transfer coefficients must be approximately equal,

$$k_D^{Fe^{3+}} \cong k_D^{Fe^{2+}} = k_D^{Fe} \tag{44}$$

since the chemical diffusivity of ferric cations and ferrous cations should be approximately the same, and the effective boundary layer thickness for both species should be the same (Equation (34)).

It is proposed that the mass transfer coefficients, $k_D^{Fe^{3+}}$ and $k_D^{Fe^{2+}}$, are high enough under these conditions that they are greater than the chemical rate constants for the two reduction reactions (Equations (3) and (4)). Of these two reduction reactions, the ferric-to-ferrous reaction must have a higher rate constant.

$$k_{Fe^{3+}\rightarrow Fe^{2+}} > k_{Fe^{2+}\rightarrow Fe} \tag{45}$$

In other words, the activation energy for the ferric-to-ferrous reaction must be smaller than that for the ferrous-to-metal reaction.

If the following relation is true:

$$k_D^{Fe} > k_{Fe^{3+}\rightarrow Fe^{2+}} > k_{Fe^{2+}\rightarrow Fe} \tag{46}$$

then with both ferric and ferrous cations present, the ferric cations will be reduced preferentially (Figure 8). This will occur because the two reduction reactions occur in

parallel, and, when mass transfer is not a problem, electrons will be consumed by whichever reaction has the higher rate constant.

It is also possible to explain the observation that ferric cations are reduced before ferrous by the following relation:

$$k_{Fe^{3+}\rightarrow Fe^{2+}} > k_D^{Fe} > k_{Fe^{2+}\rightarrow Fe}$$

Here the ferrous-to-metal reaction is chemical-reaction rate-limited, while the ferric-to-ferrous reaction is limited by mass transfer of ferric cations to the slag-metal interface. Under these conditions if both ferric and ferrous cations are present, electrons will be consumed by the ferric cations, since this gives the highest possible overall reaction rate.

To summarize, when the slag contains significant quantities of ferric cations, the overall reaction rate is limited by the rate of the ferric-to-ferrous reduction reaction. Under these conditions, the rate expression can be simplified to $r_O = k_1\left[wt.\%Fe^{3+}\right]_{slag}$, and the rate constant k_1 is essentially the chemical rate constant for the ferric-to-ferrous reduction reaction, $k_{Fe^{3+}\rightarrow Fe^{2+}}$. (See Appendix D. The rate constants.)

When the slag contains mainly ferrous oxide (i.e. very little ferric oxide), the overall reaction rate is limited by mass transfer of ferrous cations in the slag phase. Under these conditions, the rate expression is $r_O = k_2\left[wt.\%Fe^{2+}\right]_{slag}$, and the rate constant k_2 is essentially the mass transfer coefficient for ferrous cations in the slag, $k_D^{Fe^{2+}}$. (See

Appendix D. The rate constants.) If the concentration of ferrous oxide were very high, of course, it is possible that other reaction steps could become rate-limiting. For example, the flux of iron cations to the slag-metal interface could become large enough that carbon transport in metal phase, or the chemical reaction rate of ferrous-to-metal reaction might become rate-limiting.

5.3 Evidence for electrochemical mechanism

The second part of the study aimed to verify that both the reduction of iron oxide and the decarburization of liquid iron have an electrochemical component. Short-circuit experiments #1 and #2 showed that the reaction rate could be increased by penetrating the slag with an electronic conductor. This can be understood if one considers that the rate-limiting process in either the reduction of iron oxide or the decarburization of liquid iron is, under most circumstances, the mass transport of iron cations in the slag phase.

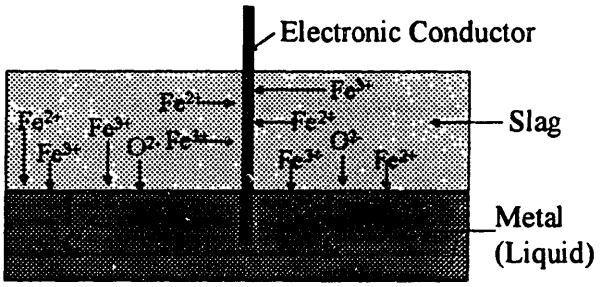

Figure 32. Iron cations in the bulk slag phase are reduced

Short-circuiting the slag layer provides a pathway for electrons, produced by the anodic reaction at the slag-metal interface, to travel far from the slag-metal interface into the bulk of the slag. Iron cations that are reduced at the interface between the slag and the short-circuit material do not have to be transported all the way to the slag-metal interface (Figure 32). In short-circuit experiment #3, the short-circuit current was actually observed experimentally. Electrons flowed from the metal bath through the external circuit to the cathode-slag interface, where they were consumed in the cathode reaction.

To increase the reaction rate further, it makes sense to apply a voltage to drive the flow of electrons from the metal bath to the cathode (Figure 33). This was done in decarburization experiments #2 and #3, and in reduction experiments #1 through #3. It was observed in these electrolysis experiments that the reaction rate could be increased by applying a voltage across the slag layer.

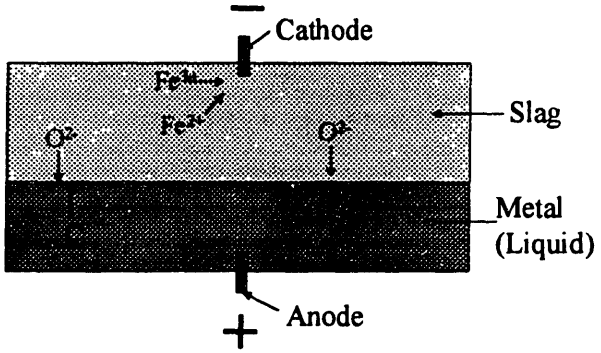

Figure 33. The reaction rate increases when current passes through the external circuit

The electrolysis experiments show that the current efficiency decreases with increasing current density (Table VII and Table VIII). At high current densities, metal will be deposited quickly at the cathode. This will lead to electronic short-circuiting of the slag layer, and to a decrease in current efficiency. It should be noted that it is also possible that a decrease in current efficiency, as we have calculated it here, could be caused by a change in the anodic reaction from that given in Equation (2) to the reversion of the

reaction in Equation (4). This would occur if the rate of mass transport of solute carbon to the slag-metal interface were too low.

Table VII. Current density and efficiency for decarburization experiments

Experiment description	Cathode type	Current (A)	Cathode-slag area* (cm^2)	Current density (A cm^{-2})	Current efficiency (%)
Decarburization experiment #2	molybdenum rod (exposed to Ar-CO_2 phase)	3.75	3.7	1	45
Decarburization experiment #3	electric arc	8	20	0.4	50

*Estimated

Table VIII. Current density and efficiency for reduction experiments

Experiment description	Cathode type	Current (A)	Cathode-slag area* (cm^2)	Current density (A cm^{-2})	Current efficiency (%)
Reduction experiment #1	molybdenum rod	2.30	3.7	0.62	36
Reduction experiment #2	electric arc	10	20	0.5	100
Reduction experiment #3	electric arc	20	20	1	75

*Estimated

5.4 Implications of this work

An important implication of this study relates to the problem of high iron oxide contents of steelmaking slags. As was mentioned in the Introduction, the original motivation for this study was to determine whether some electrochemical means involving an electric arc or plasma might be developed to increase the rate of reduction of iron oxide from

slag. In principle, three things can be done with slag from the EAF and BOF: (1) it can be returned (i.e. recycled) to the steelmaking furnace or the blast furnace; (2) it can be transferred to the ladle; and (3) it can be discarded. In practice, most slag is discarded. Recycling the slag causes the level of impurities such as phosphorus and zinc to rise[26]. Carrying over slag from the steelmaking furnace into the ladle decreases the efficiency of deoxidation with silicon and aluminum[27], since the FeO in the furnace slag dissociates slowly, releasing solute oxygen into the steel bath (i.e. the reversion of the reaction in Equation (58)).

Iron "units" are lost when steelmaking slag is discarded, since the slag contains a significant quantity of FeO. Under normal practice, the FeO level of steelmaking slag is approximately 20 wt% during the main portion of the blow, and then rises rapidly near the end of the blow levels as high at 35 or 40 wt%, depending on the final carbon content of the bath at tap. Without increasing the rate of the reaction Equation (1), it unlikely that sufficient time can be allowed in the BOF or EAF for the reaction in Equation (1) to come to equilibrium; the rate of this slag-metal reaction is relatively slow when compared to the rates of the main reactions occurring in the steelmaking furnace:

$$\frac{1}{2}(O_2) \rightarrow [wt\%\ O]_{metal} \tag{47}$$

$$[C]_{metal} + [O]_{metal} \rightarrow (CO) \tag{59}$$

If the rate of the reaction could be increased somehow, however, the iron oxide content in the slag might be held to a much lower level. The results of this thesis suggest that it may

be possible to reduce iron oxide from the slag phase at a relatively high rate if a voltage is applied across the slag layer.

Two configurations are possible. If the metal bath contains significant quantities of carbon, then the anode can contact the metal bath, and the cathode can be an electric arc or plasma torch contacting the surface of the slag layer. The anode material could be carbon, a high-melting point metal, or an electronically conductive refractory. Use of an electric arc or plasma torch would increase the cathode-slag area, which would decrease the current density, and therefore increase the current efficiency. The anodic reaction would take place at the interface between the metal bath and the slag layer; oxygen from the slag would react with carbon dissolved in the metal:

$$\left[O^{2-}\right]_{slag} + [C]_{metal} \rightarrow (CO) + 2e^{-} \tag{2}$$

The cathodic reaction would take place at the interface between the arc and the slag layer; ferrous cations would be reduced to metallic iron:

$$\left[Fe^{2+}\right]_{slag} + 2e^{-} \rightarrow [Fe]_{metal} \tag{4}$$

If the metal bath is low in carbon, then a carbon rod could be dipped in the slag layer to serve as the anode; the cathode would still be an electric arc contacting the slag layer from above. The anodic reaction would take place between solid carbon and the slag:

$$C + \left[O^{2-}\right]_{slag} \rightarrow (CO) + 2e^{-} \tag{48}$$

The cathodic reaction would take place at the interface between the arc and the slag layer; ferrous cations would be reduced to metallic iron:

$$\left[Fe^{2+}\right]_{slag} + 2e^{-} \rightarrow \left[Fe\right]_{metal} \tag{4}$$

This process could be carried out in the EAF or BOF, in some new vessel into which the steelmaking slag would be discarded, or in the ladle. The application of voltage may increase the reaction rate sufficiently to make the process viable. Conditions would have to be maintained so that iron oxide would be the least stable oxide in the slag. If the steelmaking slag contained phosphorus oxide, for example, one might reduce phosphorus oxide before iron oxide if process conditions were not maintained properly; proper conditions would be relatively low temperature, and high slag basicity.

Chapter 6. Conclusions

This study has resulted in many new findings that increase our knowledge of the slag-metal reaction between iron oxide in slag and carbon dissolved in iron. Several of the conclusions have the potential for practical application in the iron and steel industries. In the first part of the study, the reduction of iron oxide from calcia-silica-alumina slag was studied. Several significant observations were made:

- The reaction rate depended on both the ratio of ferric to ferrous cations, and the total amount of iron cations in the slag.
- When ferric and ferrous cations were both present, ferric cations were reduced preferentially.
- When the iron cations in the slag are mainly ferrous, the rate constant depended on the concentration of iron in the slag.

Based on these observations, the following conclusions have been drawn:

- The reaction rate can be modeled by a rate expression of the following form: $r_O = k_1\left[wt.\%Fe^{3+}\right]_{slag} + k_2\left[wt.\%Fe^{2+}\right]_{slag}$. Numerical values for the constants k_1 and k_2 were calculated for certain experimental conditions.
- When the slag contains significant quantities of ferric cations, the overall reaction rate is determined by the rate of the ferric-to-ferrous reduction reaction. Under these

conditions, the rate expression can be simplified to $r_O = k_1\left[wt.\%Fe^{3+}\right]_{slag}$, and the rate constant k_1 is the chemical rate constant for the ferric-to-ferrous reduction reaction.

- Starting from a slag containing both ferric and ferrous oxide, the total reaction period can be divided into two parts. In the first part, mainly ferric cations are reduced, and the concentration of ferrous oxide rises, while the total iron oxide content remains fairly constant. In the second part, ferrous cations are reduced, and both the ferrous oxide and total iron content of the slag decrease with time.
- When the slag contains mainly ferrous oxide (i.e. very little ferric oxide), the overall reaction rate is limited by mass transfer of ferrous cations in the slag phase. Under these conditions, the rate expression is $r_O = k_2\left[wt.\%Fe^{2+}\right]_{slag}$, and the rate constant k_2 is the mass transfer coefficient for ferrous cations in the slag.
- The mass transfer coefficient decreases as the concentration of ferrous oxide in the slag decreases because the rate of CO evolution decreases; as this occurs, the fluid flow conditions in the slag phase change from forced convection toward natural convection. At high concentrations, the mass transfer coefficient approaches a maximum value; the effective boundary layer thickness approaches some minimum value, δ_o.

In the second part of the study, the electrochemical nature of two reactions involving iron oxide in slag and carbon in liquid iron was studied. Several important observations were made:

- The rate of reduction of iron oxide from slag by carbon in liquid iron was increased by electrically short-circuiting the slag layer with an iron rod or plate, and the effect became more significant as the contact area between the slag and the short-circuit material increased. A small short-circuit current of approximately 80 mA was measured in two experiments.
- The rate of reduction of iron oxide from slag by carbon in liquid iron was increased by applying a voltage across the slag layer. The reaction rate increased by 60-100%, and the increase was proportional to the current passed.
- For the reduction of iron oxide with applied voltage, a current efficiency of nearly 100% was observed for current densities on the order of 500 mA cm^{-2}. The current efficiency decreased as the current density increased.
- The steady-state rate of decarburization of liquid iron by CO_2 through slag containing iron oxide was increased by applying a voltage across the slag layer.
- For decarburization with applied voltage, the current efficiency was approximately 50% for a current density on the order of 400 mA cm^{-2}. The current efficiency decreased as the current density increased.

The following conclusions have been drawn from these observations:

- The reduction of iron oxide from slag by carbon in iron occurs as separate anodic and cathodic reactions; the locations of these reactions may be physically separated by macroscopic distances.

- Short-circuiting the slag layer provides an electronically conductive pathway from the metal bath into the bulk slag phase, and allows for the reduction of iron cations located far from the slag-metal interface. When the reaction rate is limited by slag-phase mass transfer, this increases the observed reaction rate.
- Applying a voltage across the slag layer drives the flow of electrons from the metal phase to the cathode. As long as iron cations are the most easily reduced species in the slag phase, application of a voltage increases the rate of reduction of iron oxide from slag.

Chapter 7. Suggestions for Further Work

This study has shown the feasibility of increasing the rate of reduction of iron oxide from slag by "electric arc electrolysis." Further work should be done to show that this works on a larger scale. It may be possible to reduce the iron oxide content of steelmaking slag by using this method (see Chapter 5. Implications of this work).

In the laboratory, further work should be done on the reduction of other oxides from slag. McLean et al.[22] earlier suggested that it may be possible to remove unwanted impurities from metal, and to add alloying elements at a high rate by applying a voltage across the slag layer.

Appendix A. Relationships between measures of iron oxide concentration

There are several ways to express the iron oxide content of slag[28,29]. Slag analysis gives the weight percentage total iron, $[wt\%\ Fe_t]_{slag}$, and the weight percentage ferrous iron, $[wt\%\ Fe^{2+}]_{slag}$, in the slag. ("Total iron" is the slag is the sum of ferrous and ferric cations, and does not include metallic iron entrained in the slag sample.) The weight percentage ferric iron is then calculated by difference.

$$[wt\%\ Fe^{3+}]_{slag} = [wt\%\ Fe_t]_{slag} - [wt\%\ Fe^{2+}]_{slag} \tag{49}$$

The weight percentage FeO is calculated from the weight percentage ferrous iron.

$$[wt\%\ FeO]_{slag} = \frac{71.844}{55.845}[wt\%\ Fe^{2+}]_{slag} \tag{50}$$

$$[wt\%\ FeO]_{slag} \cong 1.29[wt\%\ Fe^{2+}]_{slag}$$

The weight percentage Fe_2O_3 is calculated from the weight percentage ferric iron.

$$[wt\%\ Fe_2O_3]_{slag} = \frac{159.688}{2(55.845)}[wt\%\ Fe^{3+}]_{slag} \tag{51}$$

$$[wt\%\ Fe_2O_3]_{slag} \cong 1.43[wt\%\ Fe^{3+}]_{slag}$$

In some cases the sum of FeO and Fe_2O_3 is reported, using the values calculated with Equations (50) and (51). In other cases, a value called $[wt\%\ 'FeO']_{slag}$, $[wt\%\ Fe_tO]_{slag}$, or $[wt\%\ FeO_t]_{slag}$, is calculated.

$$[wt\%\ 'FeO']_{slag} = [wt\%\ Fe_tO]_{slag} = [wt\%\ FeO_t]_{slag} \tag{52}$$

This value represents the amount of FeO that would be present if all of the iron (as represented by $[wt\%\ Fe_t]_{slag}$) were in the form of FeO.

$$[wt\%\ 'FeO']_{slag} = \frac{71.844}{55.845}\left([wt\%\ Fe^{2+}]_{slag} + [wt\%\ Fe^{3+}]_{slag}\right) \tag{53}$$

or, in terms of total iron in the slag phase,

$$[wt\%\ 'FeO']_{slag} = \frac{71.844}{55.845}[wt\%\ Fe_t]_{slag}. \tag{54}$$

$$[wt\%\ 'FeO']_{slag} \cong 1.29[wt\%\ Fe_t]_{slag}$$

Substituting Equations (50) and (51) into Equation (53) one obtains an equation for $[wt\%\ 'FeO']_{slag}$ in terms of $[wt\%\ FeO]_{slag}$ and $[wt\%\ Fe_2O_3]_{slag}$.

$$[wt\%\ 'FeO']_{slag} = [wt\%\ FeO]_{slag} + \frac{2(71.844)}{159.688}[wt\%\ Fe_2O_3]_{slag} \tag{55}$$

$$[wt\%\ 'FeO']_{slag} \cong [wt\%\ FeO]_{slag} + 0.90[wt\%\ Fe_2O_3]_{slag}$$

The oxygen associated with iron cations in slag, $[wt\%\ O]_{slag}$, is calculated with the following formula:

$$[wt\%\ O]_{slag} = \frac{15.9995}{55.845}\left([wt\%\ Fe^{2+}]_{slag} + 1.5[wt\%\ Fe^{3+}]_{slag}\right) \tag{56}$$

$$[wt\%\ O]_{slag} \cong 0.29[wt\%\ Fe^{2+}]_{slag} + 0.43[wt\%\ Fe^{3+}]_{slag}$$

Another variation, also based on the idea that the oxygen associated with iron oxide is of primary importance, is given in the following equation:

$$[wt\%\ 'FeO']_{slag} = [wt\%\ FeO]_{slag} + 1.5\frac{2(71.844)}{159.688}[wt\%\ Fe_2O_3]_{slag} \tag{57}$$

$$[wt\%\ 'FeO']_{slag} \cong [wt\%\ FeO]_{slag} + 1.35[wt\%\ Fe_2O_3]_{slag}$$

Comparison of Equations (55) and (57) shows that these two approaches will yield quite different results if the amount of ferric iron in the slag is significant.

The results of this study have been analyzed using Equation (56). This practice emphasizes that the reduction of iron oxide from slag is the removal of oxygen associated with iron cations from the slag. The value of $[wt\%\ O]_{slag}$ approaches zero as the reduction of iron oxide nears completion.

Appendix B. Concentration of FeO in slag in equilibrium with liquid Fe-C

Studies have been performed in the past on the thermodynamics and kinetics of the reaction between iron oxide in slag and carbon in iron.

$$[FeO]_{slag} + [C]_{metal} \rightarrow [Fe]_{metal} + (CO) \tag{1}$$

Equilibrium calculations for this reaction are based on studies of two simpler reactions, the oxidation of iron[30,31] and the oxidation of carbon[32],

$$[Fe]_{metal} + x[O]_{metal} \leftrightarrow [FeO_x]_{slag} \tag{58}$$

$$[C]_{metal} + [O]_{metal} \rightarrow (CO) \tag{59}$$

rather than on the actual slag-metal reaction in Equation (1). The solubility of oxygen in liquid iron over the temperature range 1530 to 1960°C is given by the following equation[31]:

$$\log_{10}[wt\%\ O]_{metal}^{saturation} = -\frac{6380}{T[K]} + 2.765 \tag{60}$$

The standard Gibbs free energy of reaction for the reaction in Equation (58) can be calculated from this data; Elliott et al.[33] give the following equation:

$$\Delta G^{\circ}\left[\frac{\text{J}}{\text{mol}}\right] = -120900 + 52.34 \cdot T[K] \tag{61}$$

The equilibrium constant for the reaction in Equation (59) is given by the following equation[32]:

$$\log_{10} K = \frac{1168}{T[K]} + 2.07 \tag{62}$$

The standard Gibbs free energy of reaction for the reaction in Equation (59) is therefore:

$$\Delta G^{\circ}\left[\frac{\mathrm{J}}{\mathrm{mol}}\right] = -22370 - 39.64 \cdot T[K] \tag{63}$$

Combining Equations (61) and (63), one finds that the standard Gibbs free energy of reaction for the reaction in Equation (1) is

$$\Delta G^{\circ}\left[\frac{\mathrm{J}}{\mathrm{mol}}\right] = 98530 - 91.98 \cdot T[K] \tag{64}$$

The reaction quotient for Equation (1) is given by the following equation

$$Q = \frac{a_{Fe} p_{CO}}{a_{FeO} a_C} \tag{65}$$

In Equation (64), the Raoultian activity scale is used for FeO in liquid slag, with concentration measured in mole fraction; the standard state is pure liquid FeO. Also, the Henrian activity scale is used for carbon in liquid iron, with concentration measured in weight percent; the standard state is a 1 wt%-solution of carbon in liquid iron. Equation (65) can therefore be written in the following form:

$$Q = \frac{p_{CO}}{\gamma_{FeO} x_{FeO} f_C [wt\%\ C]_{metal}} \tag{66}$$

The mole fraction of FeO in the slag, x_{FeO}, can be written in terms of the weight percentage of FeO, $[wt\%\ FeO]_{slag}$, and the molecular weight (relative molar mass) of FeO, M_{FeO}:

$$x_{FeO} = \frac{[wt\%\ FeO]_{slag} / M_{FeO}}{\sum_i \%i / M_i} \tag{67}$$

The term in the denominator is equal to the total number of gram-moles of oxides per 100 grams of slag, and is equal to 1.63 ± 0.09 for typical iron- and steelmaking slags (see Table IX).

For the slag used in this study, the term in the denominator of Equation (67) is equal to 1.63. The mole fraction of FeO can therefore be written more simply:

$$x_{FeO} = \frac{[wt\%\ FeO]_{slag}}{(72)(1.63)} \tag{68}$$

The value of the activity coefficient for carbon, f_C, can be determined using the appropriate first-order interaction coefficients for carbon and oxygen in liquid iron[34]:

$$\log f_C = 0.14[wt\%\ C]_{metal} - 0.34[wt\%\ O]_{metal} \tag{69}$$

The oxygen concentration is low enough to be neglected in the calculation of f_C except for steels with less than 0.05% C. (The value of $10^{-0.34[\%O]}$ is about 0.98 for 0.1% C steel, 0.97 for 0.05% C, and 0.85 for 0.01% C). The activity coefficient f_C can therefore be written in terms of $[wt\%\ C]_{metal}$:

$$f_C = 10^{0.14[wt\%\ C]_{metal}} \tag{70}$$

Table IX. Number of gram-moles of oxides per 100 grams of slag

%CaO	%MgO	%MnO	%FeO	$\%SiO_2$	$\%P_2O_5$	$\%Al_2O_3$	$\%Cr_2O_3$	$\sum_i \%i/M_i$	Type of slag
48	5	4	25	15	2	1	0	1.66	basic oxygen furnace (BOF)
53	6	5	13	20	2	1	0	1.70	BOF
60	4	3	5	25	2	1	0	1.72	BOF
24	4	3	42	10	3	10	4	1.47	electric arc furnace (EAF)
33	5	4	30	15	2	8	3	1.55	EAF
47	5	4	10	20	2	10	2	1.62	EAF
40	10	0	1	37	0	12	0	1.71	blast furnace (BF)
45	0	0	6	38	0	11	0	1.63	present study

Substituting Equations (68) and (70) into Equation (66), one obtains the following expression for the reaction quotient:

$$Q = \frac{(72)(1.63)p_{CO}}{\gamma_{FeO}[wt\%\ FeO]_{slag}\, 10^{0.14[wt\%\ C]_{metal}}[wt\%\ C]_{metal}} \tag{71}$$

If the reaction in Equation (1) is in equilibrium, then the reaction quotient, Q, is equal to the equilibrium constant, K, and the concentration of FeO in the slag is given by the following equation:

$$[wt\%\ FeO]_{slag} = \frac{(72)(1.63)p_{CO}\exp\left(\frac{11850}{T[K]} - 11.06\right)}{\gamma_{FeO}\, 10^{0.14[wt\%\ C]_{metal}}[wt\%\ C]_{metal}} \tag{72}$$

In this study, the experimental conditions were $P_{CO} = 1$ atm, $\gamma_{FeO} = 2$, $[wt\%\ C]_{metal} = 5$, and the temperature was in the range 1400°C to 1600°C. Using Equation (72), one calculates that the equilibrium concentration of FeO is 0.04 wt% at 1400°C and 0.02 wt% at 1600°C; this is 0.03 wt% Fe^{2+} at 1400°C and 0.015 wt% Fe^{2+} at 1600°C. There is a report in the literature[35] that the concentration of FeO in blast furnace slag in equilibrium with carbon-saturated iron at 1500°C is in the range 0.03-0.1%; this agrees well with the value of 0.03% given by Equation (72) using $P_{CO} = 1$ atm, $\gamma_{FeO} = 2$, $[wt\%\ C]_{metal} = 5.16$, and T=1500°C. (Note that 5.16 wt% C is the carbon concentration in graphite-saturated iron at 1500°C.)

Appendix C. State of the iron oxide-carbon relation at tap in steelmaking furnaces

The equilibrium value of $[wt\%\ FeO]_{slag}$ calculated using Equation (72) is significantly lower than the observed value of $[wt\%\ FeO]_{slag}$ in BOF and EAF steelmaking practice[1]; the iron oxide level in steelmaking slags at tap is in the range 10-25 wt% FeO for 0.1% C steel[36]. In other words, the oxygen potential in the slag, as represented by $[wt\%\ FeO]_{slag}$, is higher than the oxygen potential in the metal, as represented by $[wt\%\ O]_{metal}$. The reaction in Equation (58) is therefore not at equilibrium in industrial steelmaking furnaces. (The reaction between solute and carbon and solute oxygen in Equation (59) is close to equilibrium, however, for one atmosphere of CO[1].)

Appendix D. The rate constants

The rate constant has been calculated from the results of a number of experiments (Figure 12). The observed rate constant, k, is in the range $2 \cdot 10^{-6}$ to $1.4 \cdot 10^{-5}$ m s^{-1}. Experiments with slag sampling have shown that ferric cations are reduced initially. If one assumes that the initial CO that is produced is the result of the reduction of ferric cations to ferrous cations, then one can calculate the value of $[wt\%\ O]_{slag}$ at which the ferric cations are depleted (Table X). One can see by examining Figure 12 that most of the ferric cations are reduced to ferrous before the "transient" portion of the experiment is over. The observed rate constant, k, is therefore essentially the rate constant k_2 (Equation (43)).

Table X. Calculation of %O in slag when ferric cations are depleted

Experiment #	$[wt\%\ O]_{slag}^{initial}$ (Equation (56))	$[wt\%\ O]_{slag}$ when ferric cations are depleted
1-6	1.78	1.45
7, 10, 16	1.84	1.45
9, 17-19	5.80	4.67

The units of k_2 must be mol m^{-2} s^{-1}, but the units of k in Figure 12 are m s^{-1}. One can calculate the value of k_2 from the corresponding value of k. The rate constant k is used in a rate expression of the following form:

$$r\left[\frac{\text{mol}}{\text{m}^2\,\text{s}}\right] = k\left[\frac{\text{m}}{\text{s}}\right] c_{Fe^{2+}}\left[\frac{\text{mol}}{\text{m}^3}\right] \tag{73}$$

The concentration of ferrous cations in molar units is related to the weight percentage of ferrous cations

$$c_{Fe^{2+}}\left[\frac{\text{mol}}{\text{m}^3}\right]=\frac{\left[wt\%\ Fe^{2+}\right]_{slag}}{100}\frac{\rho_{slag}\left[\frac{\text{kg}}{\text{m}^3}\right]}{55.845\cdot 10^{-3}\left[\frac{\text{kg}}{\text{mol}}\right]} \tag{74}$$

where ρ_{slag} is the density of the slag. Substituting Equation (74) into Equation (73) one obtains a rate expression in terms of $\left[wt\%\ Fe^{2+}\right]_{slag}$.

$$r\left[\frac{\text{mol}}{\text{m}^2\ \text{s}}\right]=k\left[\frac{\text{m}}{\text{s}}\right]\frac{\left[wt\%\ Fe^{2+}\right]_{slag}}{100}\frac{\rho_{slag}\left[\frac{\text{kg}}{\text{m}^3}\right]}{55.845\cdot 10^{-3}\left[\frac{\text{kg}}{\text{mol}}\right]} \tag{75}$$

When only ferrous cations are present, Equation (43) reduces to

$$r=k_2\left[wt\%\ Fe^{2+}\right]_{slag} \tag{76}$$

Comparing Equations (75) and (76) one sees the relation between k_2 and k.

$$k_2\left[\frac{\text{mol}}{\text{m}^2\ \text{s}}\right]=k\left[\frac{m}{s}\right]\frac{\rho_{slag}\left[\frac{\text{kg}}{\text{m}^3}\right]}{5.5845} \tag{77}$$

Since k is in the range $2\cdot 10^{-6}$ to $1.4\cdot 10^{-5}$ m s^{-1} (Figure 12), k_2 is in the range $9\cdot 10^{-4}$ to $6.3\cdot 10^{-3}$ mol m^{-2} s^{-1}, assuming the slag density is 2500 kg m^{-3}.

The rate constant k_1 can be estimated from slag analysis results. During experiment #10 (Table III), the slag initially contained 2.66 wt% Fe^{2+} and 2.35 wt% Fe^{3+}. The first sample, taken 15 minutes after the slag was added to the crucible, contained 4.43 wt%

Fe^{2+} and 0.23 wt% Fe^{3+}. One calculates that the reaction rate in terms of CO using the Fe^{2+} values is 0.011 mol CO m^{-2} s^{-1}. Using the Fe^{3+} values, one calculates that the reaction rate is 0.013 mol CO m^{-2} s^{-1}. When the concentration of ferric cations is significant, Equation (43) reduces to

$$r_{CO} = k_1 \left[wt.\% Fe^{3+} \right]_{slag} \tag{78}$$

(It is assumed that the rate in terms of oxygen is equal to the rate in terms of CO.) Using Equation (78), a reaction rate of 0.012 mol CO m^{-2} s^{-1}, and the average concentration of Fe^{3+} over the 15 minutes (i.e. 1.29 wt% Fe^{3+}), one calculates that k_1 is $9.3 \cdot 10^{-3}$ mol m^{-2} s^{-1}.

Appendix E. Carbon concentration during short circuit experiments #1 and #2

The mass of the complete rod-and-plate combination was approximately 743 g. During short-circuit experiment #1, the whole flag melted into the metal bath. Since the original metal mass was 605 g (Table IV), the final mass of metal was 1348 g. The original concentration of carbon was approximately 5 wt%, so the final concentration was 0.05(605)/1348 = 2.2 wt% C.

During short-circuit experiment #2, the plate and a portion of the rod melted into the metal bath. The original mass of the steel flag was 743 g, and the mass after the lower portion melted off was 516 g. Since the metal mass in the crucible was initially 772 g, the final mass of metal was 999 g. The original concentration of carbon in the bath was approximately 5 wt%, so the final concentration was 0.05(772)/999 = 3.9 wt% C.

The results of Krishna et al.[18] show that for the reduction of iron oxide (8.4 wt% FeO initially) from 47%CaO-41%SiO_2-12%Al_2O_3 base slag at 1450°C by carbon in liquid iron, the initial reaction rate is independent of the carbon concentration in the range 1.3 to 2.2 wt% C. Upadhya et al.[15] demonstrated that for the reduction of iron oxide (2.0 wt% FeO initially) from 38%CaO-42%SiO_2-20%Al_2O_3 base slag at 1410°C by carbon in liquid iron, the rate constant is independent of carbon concentration in the range 2.5 to 4.6 wt% C. These two studies suggest that, even after the iron flag melted into the liquid iron bath, the carbon concentration was high enough so that the reaction rate was still

limited by mass transport of iron oxide in the slag phase, rather than by mass transport of solute carbon in the metal phase.

Appendix F. Flux of CO in decarburization experiment #1

If the CO_2 entering the inner furnace chamber were fully converted to CO (i.e. 2 mol CO evolved per mol CO_2 fed to the inner chamber), then the rate of CO evolution would be approximately $2.1 \cdot 10^{-4}$ mol CO s^{-1}, or $3.9 \cdot 10^{-2}$ mol CO m^{-2} s^{-1}. The observed rate of CO evolution was more than an order of magnitude less than this, so there was excess CO_2 for decarburization of the metal bath.

Appendix G. Contact time

When slag that contains ferrous oxide contacts liquid iron containing a high concentration of carbon, the two react, forming CO. One can analyze this process in detail by considering a small volume element of slag in contact with a small area on the slag-metal interface. (The following derivation is based on Higbie's penetration model[37,38].) Imagine that at $t = 0$, "fresh" slag makes contact with the interface at the location under observation. For a CO bubble to form, a supersaturation of solute oxygen must develop in the metal phase. Then solute carbon and solute oxygen can react to form CO.

$$[C]_{metal} + [O]_{metal} \rightarrow (CO) \tag{79}$$

The degree of supersaturation required depends on the barrier to nucleation of a CO bubble. For homogenous nucleation in the metal bath, the supersaturation is probably the highest. The required supersaturation is probably lower for homogenous nucleation at the slag-metal interface, since the bubble can form mainly in the slag phase. (The surface tension of slag is significantly lower than the surface tension of liquid iron.) The supersaturation may be even lower for heterogeneous nucleation at a site on the crucible-metal interface, if their are cracks or pores of significant size in the crucible.

Consider the period between when the slag just makes contact with the metal, at $t = 0$, and when a CO bubble stirs the location on the slag-metal interface under observation, at $t = \theta$. This stirring could result from several phenomena: (1) a CO bubble may be released from the slag-metal interface at some location near the location under

observation; (2) a CO bubble may evolve from the bulk metal phase and pass through the slag-metal interface at the location under observation; and (3) a CO bubble may be released from some site on the crucible-metal interface and pass through the slag-metal interface at the location under observation. During the period between $t = 0$ and $t = \theta$, the overall reaction is the dissociation of ferrous oxide.

$$[FeO]_{slag} \rightarrow [Fe]_{metal} + [O]_{metal} \tag{80}$$

Since the compound FeO does not actually exist in the slag phase, this reaction (Equation (80)) must comprise two reactions: the anodic reaction

$$\left[O^{2-}\right]_{slag} \rightarrow [O]_{metal} + 2e^{-}, \tag{81}$$

and the reduction of ferrous cations (Equation (4)).

The results of this study indicate that the overall rate of reduction of iron oxide is limited by the diffusion of ferrous cations to the slag-metal interface when only ferrous oxide remains in the slag (i.e. no ferric oxide). Therefore, a concentration gradient of ferrous cations must develop in the slag layer adjacent to the slag-metal interface during the period between $t = 0$ and $t = \theta$. This gradient is a "local" one (i.e. at the location under observation), as opposed to the "overall" or "effective" gradient that was discussed earlier (and pictured in Figure 31).

The local gradient in ferrous cations varies with position on the slag-metal interface. At some moment, the slag at one location on the slag-metal interface may be high in ferrous cations, while the slag at some other location may be low. The longer a volume

"element" of slag remains in contact with the interface, the more highly depleted in ferrous cations it becomes.

One can calculate the flux of ferrous cations toward the slag-metal interface as a function of time during the period between $t = 0$ and $t = \theta$. Let x be the direction perpendicular to the slag-metal interface, with $x = 0$ at the interface, and $x > 0$ in the slag phase. This is a one-dimensional transient diffusion problem, so one must solve

$$\frac{dc}{dt} = -\frac{dJ}{dx}, \tag{82}$$

which is derived from a mass balance on a volume element Adx, for the flux of ferrous cations, J. (The flux is positive if it is in the positive x direction.) Using Fick's first law, one can write the flux, J, in terms of the concentration gradient and the chemical diffusivity of ferrous cations, D.

$$J = -D\frac{dc}{dx} \tag{83}$$

Substituting Equation (83) into Equation (82), and assuming that the diffusivity is constant, one obtains Fick's second law.

$$\frac{dc}{dt} = D\frac{d^2c}{dx^2} \tag{84}$$

At $t = 0$, the concentration of ferrous cations is equal to the current concentration in the bulk slag phase.

$$c(x, t = 0) = c_{bulk} \tag{85}$$

At $0 < t < \theta$, the concentration of ferrous cations at the slag-metal interface ($x = 0$) is essentially given by Equation (72), since equilibrium is established as the interface.

$$c(x = 0, t) = c_{interface} = c_{equilibrium} \tag{86}$$

The concentration far from the interface is equal to the concentration in the bulk slag phase.

$$\lim_{x \to \infty} c(x, t) = c_{bulk} . \tag{87}$$

The solution to Equation (84), given the initial condition in Equation (85) and the boundary conditions in Equations (86) and (87), can be written in terms of the error function.

$$c(x, t) = \left(c_{bulk} - c_{interface}\right) \mathrm{erf}\left(\frac{x}{2\sqrt{Dt}}\right) + c_{interface} \tag{88}$$

Substituting Equation (88) into Equation (83) and differentiating, one obtains an expression for the flux, J, of ferrous cations to the slag-metal interface.

$$J(x, t) = -\sqrt{\frac{D}{\pi \cdot t}} \cdot \left(c_{bulk} - c_{interface}\right) \cdot \exp\left(-\frac{x^2}{4Dt}\right) \tag{89}$$

The flux is negative since ferrous cations are diffusing in the negative x direction (i.e. toward the slag-metal interface from the bulk slag phase). Note that the flux varies with position, x, and time, t. At a given value of x, the flux decreases with time, as the concentration profile (of ferrous cations) develops. The time-averaged flux at a given value of x is given by the following expression:

$$\left\langle J(x,\theta)\right\rangle = \frac{\int_{t=0}^{t=\theta} -\sqrt{\frac{D}{\pi \cdot t}} \cdot \left(c_{bulk} - c_{interface}\right) \cdot \exp\left(-\frac{x^2}{4Dt}\right) dt}{\int_{t=0}^{t=\theta} dt} \tag{90}$$

The time-averaged flux depends on the parameter, θ, used in the integration. For $x = 0$, Equation (90) takes the form

$$-\left\langle J(0,\theta)\right\rangle = \sqrt{\frac{4D}{\pi\theta}}\left(c_{bulk} - c_{interface}\right), \tag{91}$$

in which the flux is proportional to the difference in ferrous cation concentration between the bulk slag phase and the slag at the slag-metal interface. The flux in Equation (91) is the time-average flux at a single location. One can only observe a flux that is both position-averaged and a time-averaged:

$$-\left\langle \left\langle J(0,\theta)\right\rangle_{time} \right\rangle_{position} = \sqrt{\frac{4D}{\pi\left\langle\theta\right\rangle_{position}}}\left(\left\langle c_{bulk}\right\rangle_{position} - \left\langle c_{interface}\right\rangle_{position}\right) \tag{92}$$

This flux, on the left-hand side of Equation (92), is the same as that on the left-hand side of Equation (24). (The concentrations on the right-hand side of Equations (92) and (24) are position-averaged, as opposed to local concentrations at some point on the slag-metal interface.) Comparison of Equations (92) and (24) shows that this derivation leads to the relation

$$k_D = \sqrt{\frac{4D}{\pi\left\langle\theta\right\rangle_{position}}}, \tag{93}$$

which was discussed in Chapter 5 (see Equation (31)). The contact time, θ, in Equation (31) is equal to the position-averaged parameter, θ, in Equation (93). The contact time is

therefore the position-averaged time between CO bubbles' stirring the slag-metal interface.

It is interesting to calculate the contact time implied by the observed values of the mass transfer coefficient (rate constant). The data in Figure 12 show that the mass transfer coefficient was as high as $1.4 \cdot 10^{-5}$ m s^{-1} under some conditions. For this value of k_D, and using a value of $0.35 \cdot 10^{-9}$ m^2 s^{-1} for the chemical diffusivity, D, of ferrous cations in the slag[39], one calculates that θ is equal to 2.3 seconds. For $k_D = 2.0 \cdot 10^{-6}$ m s^{-1} and $D = 0.35 \cdot 10^{-9}$ m^2 s^{-1}, one calculates that $\theta = 110$ s.

Appendix H. Analysis of results using dimensionless numbers

Experimental results of studies on mass transfer are often analyzed using dimensionless quantities. The following correlation has been used previously[40] to relate the Nusselt number to the Reynolds number and the Schmidt number.

$$Nu = b \cdot Re^m Sc^n \tag{94}$$

The quantities b, m, and n are empirical constants. The Nusselt number for mass transfer, also called the Sherwood number, is related to the mass transfer coefficient, k_D, the characteristic length, L, and the mass diffusivity, D.

$$Nu = \frac{k_D L}{D} \tag{95}$$

The Reynolds number is related to the velocity of the fluid in the bulk, u_{bulk}, the characteristic length, L, and the kinematic viscosity of the fluid, ν.

$$Re = \frac{u_{bulk} L}{\nu} \tag{96}$$

The Schmidt number is related to the properties of the fluid, and is the mass transfer-analogue of the Prandtl number.

$$Sc = \frac{\nu}{D} \tag{97}$$

Substituting Equations (95), (96), and (97) into Equation (94), one obtains the following equation for the mass transfer coefficient:

$$k_D = b u_{bulk}^m L^{m-1} \nu^{n-m} D^{1-n} \tag{98}$$

For the reduction of iron oxide from slag by carbon in iron,

$$[FeO]_{slag} + [C]_{metal} \rightarrow [Fe]_{metal} + (CO). \quad (1)$$

the evolved CO stirs the slag layer, and the velocity of the fluid in the bulk, u_{bulk}, must be related to the rate of evolution of CO, r_{CO}.

$$u_{bulk} = b' r_{CO} \frac{RT}{P} \quad (99)$$

where b' is a constant, T is the temperature, and P is the pressure. Substitution of Equation (99) into Equation (98) yields the following expression for the mass transfer coefficient:

$$k_D = b\left(b' r_{CO} \frac{RT}{P}\right)^m L^{m-1} \nu^{n-m} D^{1-n} \quad (100)$$

For given experimental conditions, a plot of the natural logarithm of the rate constant, k, (interpreted by the author as the mass transfer coefficient, k_D) versus the natural logarithm of the reaction rate in terms of CO, r_{CO}, should have a slope equal to the constant m. This has been done for two typical experiments in the first part of this study (Figure 34). For experiment #6, one finds that m is 0.57 (correlation parameter $r^2 = 0.92$). For experiment #9, m is 0.62 ($r^2 = 0.95$). Richardson et al.[41] pointed out previously that most mass transfer data available for gas-stirred, liquid-liquid interfaces show that the mass transfer coefficient, k_D, is proportional to square root of the total gas flow rate, Q,

$$k_D \propto Q^{0.5} \quad (101)$$

which implies that m is equal to 0.5.

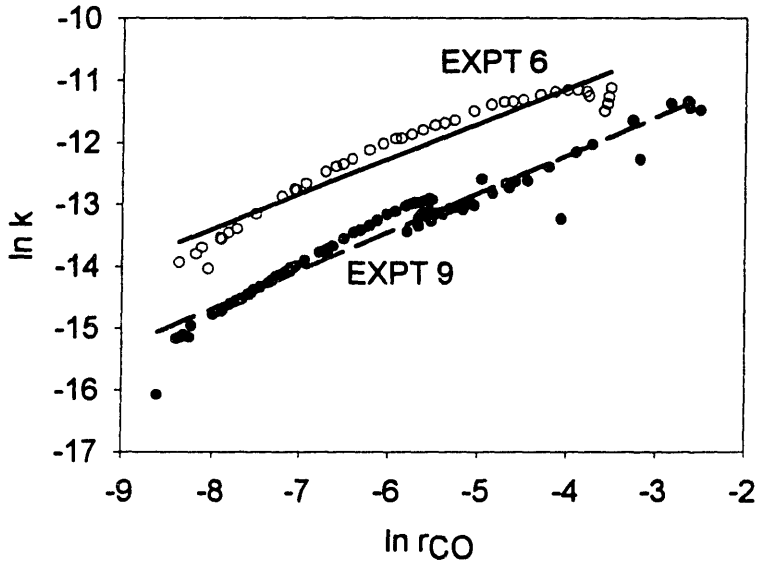

Figure 34. Plot of natural log of k_D *vs.* natural log of r_{CO} to obtain m

If the reaction rate (in terms of CO) is limited by the flux of ferrous cations to the slag-metal interface, then the rate of CO evolution is given by the following equation:

$$r_{CO} = k_D c_{Fe^{2+}}^{bulk} = k_D c \tag{102}$$

where $c_{Fe^{2+}}^{bulk} = c$ is the concentration of ferrous cations in the bulk slag phase. Substitution of Equations (102) into Equation (100) yields the following equation for the mass transfer coefficient:

$$k_D = b^{\frac{1}{1-m}} \left(\frac{b' RT}{P} \right)^{\frac{m}{1-m}} c^{\frac{m}{1-m}} L^{-1} \nu^{\frac{n-m}{1-m}} D^{\frac{1-n}{1-m}} \tag{103}$$

For given experimental conditions, a plot of the natural logarithm of the rate constant (i.e. mass transfer coefficient) versus the natural logarithm of the concentration should have a slope equal to $\frac{m}{1-m}$. This has been done for two typical experiments in the first part of this study (Figure 35). For experiment #6, one finds that the slope is 1.04 (correlation parameter $r^2 = 0.68$), which implies that m is 0.51. For experiment #9, the slope is 1.33 ($r^2 = 0.73$), which implies that m is 0.57. (The observed mass transfer coefficient has been plotted versus %O in the slag, which is equivalent to wt% Fe^{2+}, since only ferrous cations remained during the portion of data from which the slope is derived.)

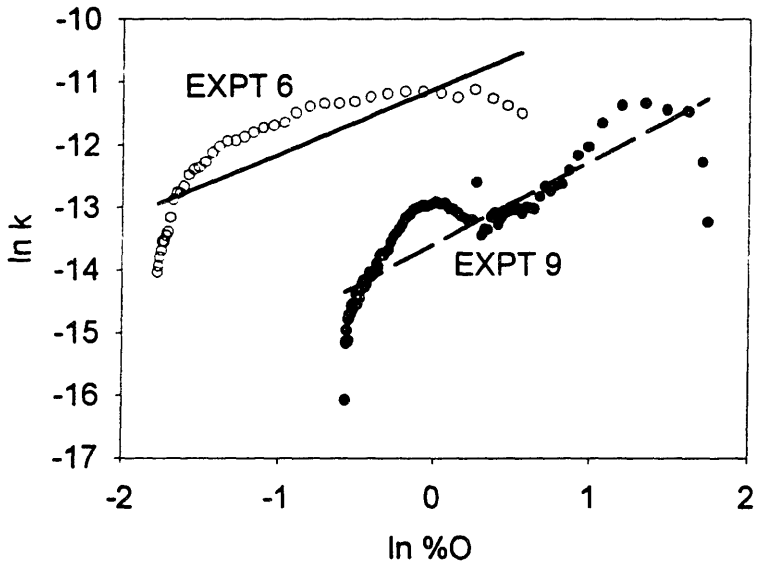

Figure 35. Plot of natural log of k_D *vs.* natural log of %O to obtain m

Appendix I. Base slag

In this study a "base slag" composition of 48 wt% calcia (CaO), 40 wt% silica (SiO_2), and 12 wt% alumina (Al_2O_3) was used. Between 5 and 16 wt% Fe was added to the slag as iron oxide (Table III). This base slag composition was selected for the following reasons:

- It resembles the slag used in the blast furnace (BF), so the reaction rate measurements may be of some practical use; this slag may be used in the future in smelting reduction (also known as direct smelting or direct ironmaking) processes.
- It is a convenient slag for laboratory purposes, since it has a low melting point (1310-1320°C) and low viscosity (5 P, or 0.5 Pa s, at 1400°C).
- It has been studied by many other researchers, so its thermodynamic and physical properties are relatively well-known.
- A number of studies have been published on the reaction rate between iron oxide in slags with compositions similar to this one and either carbon in liquid iron[5,6,16,18] or solid carbon[42,43,44]. The results of this study may be compared with the results of these other studies.

The basicity, B, of the base slag composition used in this study is 1.0, where B is calculated using the weight percentages of the constituent oxides[45].

$$B = \frac{\%CaO + 1.4(\%MgO)}{\%SiO_2 + 0.84(\%P_2O_5) + 0.60(\%Al_2O_3)} \qquad (104)$$

(Note that Equation (104) is based on the following assumptions:

- one mole of MgO is equivalent to one mole of CaO;
- one mole of P_2O_5 is equivalent to two moles of SiO_2;
- one mole of Al_2O_3 is equivalent to one mole of SiO_2.)

The viscosity of CaO-MgO-FeO-Al_2O_3-SiO_2 melts is a single function of the quantity $x_{SiO_2} + x_a$, the sum of the mole fraction of silica in the slag and the silica equivalence of the mole fraction of Al_2O_3 in the slag[46]. In slags containing less that 20 wt% Al_2O_3, the silica equivalence of Al_2O_3 is approximately equal to the mole fraction of Al_2O_3.

$$x_a \cong x_{Al_2O_3} \tag{105}$$

For the base slag composition, $x_{SiO_2} + x_a = 0.48$, and the viscosity at 1500°C is approximately 0.32 Pa s (3.2 P). Adding iron oxide to the slag decreases the viscosity[46] (Table XI); with 15 wt% FeO, the viscosity is approximately 0.21 Pa s (2.1 P). For comparison, the viscosity of water at 25°C is 0.89 mPa s; the slag used in this study is approximately 300 times more viscous than water at room temperature. The viscosity of liquid iron[47] containing 5 wt% C at 1500°C is approximately 5.3 mPa s; the slag phase in this study is approximately 50 times more viscous that the liquid metal phase. The viscosity decreases with increasing temperature. The viscosity of slag with $x_{SiO_2} + x_a = 0.45$ is given in Table XII as a function of temperature[46,48].

Table XI. Effect of iron oxide on viscosity of slag

%CaO	$\%SiO_2$	$\%Al_2O_3$	%FeO	$x_{SiO_2} + x_a$	Viscosity at 1500°C (Pa s)
48	40	12	0	0.48	0.32
47	39	12	2	0.47	0.28
46	38	11	5	0.45	0.26
43	36	11	10	0.44	0.25
41	34	10	15	0.41	0.21

Table XII. Effect of temperature on viscosity of slag

Temperature (°C)	Viscosity* (Pa s)
1400	0.5
1500	0.3
1600	0.2

*Estimated for slag with $x_{SiO_2} + x_a = 0.45$

A comparison of the base slag used in this study to slags used in iron- and steelmaking (Table XIV) shows that the base slag used herein is relatively acidic (and therefore relatively viscous). Alumina crucibles were used to contain the slag during the experiments. For simplicity, the base slag did not contain any magnesia (MgO). In contrast, blast furnace slag typically has about 10% MgO. Steelmaking slags also contain significant quantities of MgO (to minimize corrosion of MgO refractories).

Table XIV. Properties of typical iron- and steelmaking slags

Slag	%CaO	%MgO	$\%SiO_2$	$\%Al_2O_3$	(%Fe)	(%'FeO')*	$x_{SiO_2} + x_a$	B**
Blast Furnace[49]	40	10	38	12	0.8	1	0.44	1.2
Basic Oxygen Furnace (BOF)[50]	67	8	25	0	5-35	6.5-45	0.23	3.1
Electric Arc Furnace (EAF)[51]	57	6	27	10	10-40	13-52	0.32	2.0
Direct Smelting Process[52]	43	12	35	10	1.5-5	2-6	0.39	1.5
Present study	48	0	40	12	5-16	6-21	0.48	1.0

Note: the weight percentages for the oxides other than FeO sum to 100 wt%.

*Calculated using Equation (54).

**Calculated using Equation (104), not including FeO content of the slag.

Bibliography

[1] E. T. Turkdogan: *Physical Chemistry of High Temperature Technology*, Academic Press, New York, 1980, p. 368-371.

[2] W. T. Lankford, Jr., N. L. Samways, R. F. Craven, and H. E. McGannon, Editors, *The Making, Shaping and Treating of Steel*, Tenth Edition, United States Steel and the Association of Iron and Steel Engineers, Pittsburgh, PA, 1985, pp. 470-471.

[3] A. I. van Hoorn, J. T. van Konynenburg, and P. J. Kreyger, "Evolution of Slag Composition and Weight during the Blow," in *McMaster Symposium on Iron and Steelmaking No. 4: Role of Slag in Basic Oxygen Steelmaking Processes*, McMaster University Press, Hamilton, Ontario, 1979, pp. 2-1 to 2-26.

[4] W. T. Lankford, Jr., N. L. Samways, R. F. Craven, and H. E. McGannon, Editors, *The Making, Shaping and Treating of Steel*, Tenth Edition, United States Steel, 1985, pp. 529-533.

[5] W. O. Philbrook and L. D. Kirkbride, "Rate of FeO Reduction from a CaO-SiO_2-Al_2O_3 Slag by Carbon Saturated Iron," *Transactions of the Metallurgical Society of AIME*, volume 206, 1956, pp. 351-356.

[6] S. K. Tarby and W. O. Philbrook, "The Rate and Mechanism of the Reduction of FeO and MnO from Silicate and Aluminate Slags by Carbon-Saturated Iron," *Transactions of the Metallurgical Society of AIME*, volume 239, 1967, pp. 1005-1017.

[7] E. W. Mulholland, G. S. F. Hazeldean, and M. W. Davies, "Visualization of Slag-Metal Reactions by X-Ray Fluoroscopy: Decarburization in Basic Oxygen Steelmaking," *Journal of The Iron and Steel Institute*, volume 211, issue 9, September 1973, pp. 632-639.

[8] G. G. Krishna Murthy, A. Hasham, and U. B. Pal, "Reduction Rates of FeO in CaO-SiO_2-Al_2O_3-X Slags by Fe-C Droplets," *Ironmaking and Steelmaking*, volume 20, number 3, 1993, pp. 191-200.

[9] J. Szekely, U. B. Pal, and H. R. Larson, "Environmentally Conscious Plasma Arc Processes for Enhanced Metal Production," Proposal to the National Science Foundation, July 1995, pp. 1-19.

[10] T. Gare and G. S. F. Hazeldean, "Basic Oxygen Steelmaking: Decarburization of Binary Fe-C Droplets and Ternary Fe-C-X Droplets in Ferruginous Slags," *Ironmaking and Steelmaking*, volume 8, number 4, 1981, pp. 169-181.

[11] D. J. Min and R. J. Fruehan, "Rate of Reduction of FeO in Slag by Fe-C Drops," *Metallurgical Transactions B*, volume 23B, February 1992, pp. 29-37.

[12] G. G. Krishna, Y. Sawada, and J. F. Elliott, "Reduction of FeO Dissolved in CaO-SiO_2-Al_2O_3 Slags by Fe-C Droplets," *Ironmaking and Steelmaking*, volume 20, number 3, 1993, pp. 179-190.

[13] C. Wagner, "Kinetic Problems in Steelmaking," in *The Physical Chemistry of Steelmaking*, J. F. Elliott, Editor, The Technology Press and John Wiley and Sons, New York, 1958, pp. 237-251.

[14] I. D. Sommerville, P. Grieveson, and J. Taylor, "Kinetics of Reduction of Iron Oxide in Slag by Carbon in Iron: Part 1 Effect of Oxide Concentration," *Ironmaking and Steelmaking*, volume 7, number 1, 1980, pp. 25-32.

[15] K. Upadhya, I. D. Sommerville, and P. Grieveson, "Kinetics of Reduction of Iron Oxide in Slag by Carbon in Iron: Part 2 Effect of Carbon Content of Iron and Silica Content of Slag," *Ironmaking and Steelmaking*, volume 7, number 1, 1980, pp. 33-36.

[16] A. Sato, G. Aragane, F. Hirose, R. Nakagawa, and S. Yoshimatsu, "Reducing Rate of Iron Oxide in Molten Slag by Carbon in Molten Iron," *Transactions ISIJ*, volume 24, 1984, pp. 808-815.

[17] P. Wei, M. Sano, M. Hirasawa, and K. Mori, *ISIJ International*, volume 31, number 4, 1991, pp. 358-365.

[18] G. G. Krishna Murthy, A. Hasham, and U. B. Pal, "Removal of FeO During Foaming of CaO-SiO_2-Al_2O_3-FeO Slags by Low-Carbon Iron Melts," *ISIJ International*, volume 34, number 5, 1994, pp. 408-413.

[19] R. K. Paramguru, H. S. Ray, and P. Basu, *Ironmaking and Steelmaking*, volume 23, number 4, 1996, pp. 328-334.

[20] U. Pal, T. Debroy, and G. Simkovich, "Electronic and Ionic Transport in Liquid PbO-SiO_2 Systems," *Metallurgical Transactions B*, volume 16B, March 1985, pp. 77-82.

[21] M. Grimble, R. G. Ward, and D. J. Williams, "Kinetics of Silica Reduction by Carbon-Saturated Iron," *Journal of the Iron and Steel Institute*, volume 203, number 3, March 1965, pp. 264-267.

[22] A. McLean, I. D. Sommerville, and F. L. Kemeny, "Enhanced Slag-Metal Reactions," *4th International Conference on Molten Slags and Fluxes*, ISIJ, Sendai, Japan, 1992, pp. 268-273.

[23] Dulski, T. R., "Classical Wet Analytical Chemistry," in *ASM Handbook*, Volume 10 (Materials Characterization), ASM International, 1986, pp. 161-180.

[24] Furman, N. H., Editor, *Standard Methods of Chemical Analysis*, Sixth Edition, Volume I, D. Van Nostrand, Princeton, NJ, 1962, pp. 529-555.

[25] Kenner, C. T., *Laboratory Directions for Analytical Separations and Determinations*, The Macmillan Company, New York, 1971, pp. 83-85.

[26] W. T. Lankford, Jr., N. L. Samways, R. F. Craven, and H. E. McGannon, Editors, *The Making, Shaping and Treating of Steel*, Tenth Edition, United States Steel, 1985, p. 338.

[27] E. T. Turkdogan: *Fundamentals of Steelmaking*, Institute of Materials, London, 1996, p. 257.

[28] W. O. Philbrook and M. B. Bever, *Basic Open Hearth Steelmaking*, Second Edition, The American Institute of Mining and Metallurgical Engineers, New York, 1951, pp. 195-196.

[29] G. A. Meszaros, D. K. Docktor, R. P. Stone, C. J. Carr, F. L. Kemeny, L. J. Lawrence, E. T. Turkdogan, "Implementation of a Ladle Slag Oxygen Activity Sensor to Optimize Ladle Slag Practices at the U. S. Steel Mon Valley Works," *Iron and Steelmaker*, July 1997, pp. 33-39.

[30] C. R. Taylor and J. Chipman, "Equilibria of Liquid Iron and Simple Basic and Acid Slags in a Rotating Induction Furnace," *Transactions of the Metallurgical Society of AIME*, volume 154, 1943, pp. 228-247.

[31] P. A. Distin, S. G. Whiteway, and C. R. Masson, "Solubility of Oxygen in Liquid Iron from 1785°C to 1960°C. A New Technique for the Study of Slag-Metal Equilibria," *Canadian Metallurgical Quarterly*, volume 10, number 1, 1971, pp. 13-18.

[32] T. Fuwa and J. Chipman, "The Carbon-Oxygen Equilibria in Liquid Iron," *Transactions of the Metallurgical Society of AIME*, volume 218, 1960, pp. 887-891.

[33] J. F. Elliott, M. Gleiser, and V. Ramakrishna, *Thermochemistry for Steelmaking*, Volume II, Addison-Wesley, Reading, MA, 1963, p. 618.

[34] G. K. Sigworth and J. F. Elliott, "The Thermodynamics of Liquid Dilute Iron Alloys," *Metal Science*, volume 8, 1974, pp. 298-310.

[35] G. G. Hatch and J. Chipman, "Sulfur Equilibria between Iron Blast Furnace Slags and Metal," *Transactions of the Metallurgical Society of AIME*, volume 185, 1949, pp. 274-284.

[36] E. T. Turkdogan: *Fundamentals of Steelmaking*, Institute of Materials, London, 1996, pp. 232-233 and p. 241.

[37] R. Higbie, "The Rate of Absorption of a Pure Gas into a Still Liquid during Short Periods of Exposure," *Transactions of the American Institute of Chemical Engineers*, volume XXXI, D. Van Nostrand, New York, 1936, pp. 365-389.

[38] P. V. Danckwerts, "Significance of Liquid-Film Coefficients in Gas Absorption," *Industrial and Engineering Chemistry*, volume 43, number 6, pp. 1460-1467.

[39] L. Yang and G. Derge, "General Considerations of Diffusion in Melts of Metallurgical Interest," in *Physical Chemistry of Process Metallurgy*, Part 1, Edited by G. R. St. Pierre, Interscience, New York, 1961, pp. 503-521.

[40] L. J. Fister and T. B. King, "Kinetics of Reactions between Two Liquid Phases," in *Physical Chemistry of Process Metallurgy*, Part 1, Edited by G. R. St. Pierre, Interscience, New York, 1961, pp. 543-558.

[41] F. D. Richardson, D. G. C. Robertson, and B. B. Staples, "Mass Transfer Across Metal-'Slag' Interfaces Stirred by Bubbles," *Physical Chemistry in Metallurgy: Proceedings of the Darken Conference*, Edited by R. M. Fisher, R. A. Oriani, and E. T. Turkdogan, U. S. Steel, Monroeville, PA, 1976, pp. 25-48.

[42] M. Sugata, T. Sugiyama, and S. Kondo, "Reduction of Iron Oxide in Molten Slags with Solid Carbon," *Transactions ISIJ*, volume 14, 1974, pp. 88-95.

[43] J. Mróz, "Reduction of Iron Oxides from Liquid Slags with Solid Carbon," *Scandinavian Journal of Metallurgy*, volume 23, issue 4, August 1994, pp. 171-183.

[44] B. Sarma, A. W. Cramb, and R. J. Fruehan, "Reduction of FeO in Smelting Slags by Solid Carbon: Experimental Results," *Metallurgical and Materials Transactions B*, volume 27B, October 1996, pp. 717-730.

[45] E. T. Turkdogan: *Fundamentals of Steelmaking*, Institute of Materials, London, 1996, pp. 140-141.

[46] ibid., pp. 172-176.

[47] ibid., p. 133.

[48] E. T. Turkdogan, *Physicochemical Properties of Molten Slags and Glasses*, The Metals Society, London, 1983, pp. 21-25.

[49] W. T. Lankford, Jr., N. L. Samways, R. F. Craven, and H. E. McGannon, Editors, *The Making, Shaping and Treating of Steel*, Tenth Edition, United States Steel, 1985, p. 334.

[50] E. T. Turkdogan: *Fundamentals of Steelmaking*, Institute of Materials, London, 1996, pp. 219-220.

[51] ibid., pp. 240-241.

[52] B. Sarma and R. J. Fruehan, "Bath Smelting Slag Reactions," *Proceedings of the 5th International Conference on Molten Slags, Fluxes, and Salts* (Sydney, Australia), Iron and Steel Society, 1996, pp. 357-374.

Biographical Note

The author graduated from MIT in June, 1993 with a bachelor of science (S.B.) degree in materials science and engineering, and in September, 1993 with an S.B. in mathematics. He worked with Professor Julian Szekely from June, 1993 until October, 1995 in Szekely's Materials Process Modeling Group, and with Professor Uday Pal from October, 1995 until January, 1998 in Pal's High Temperature Materials Process Technology Group. After graduation, the author will be a visiting scientist at Boston University in the Department of Manufacturing Engineering.